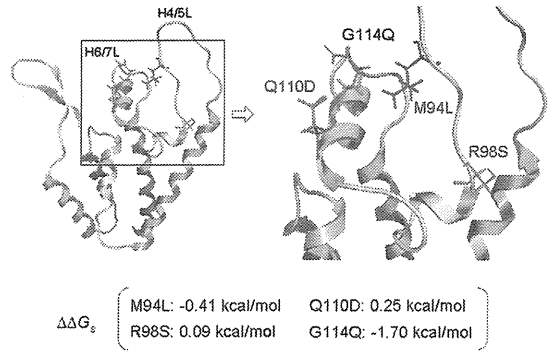

FIG 3 Structural analysis of the HIV-1mt CA NTD. A molecular model of the HIV-1mt CA NTD was constructed by homology modeling and refined as described previously (19). Single-point mutations were generated on the CA model, and ensembles of protein conformations were generated by using the LowMode MD module in MOE (Chemical Computing Group Inc., Quebec, Canada) to calculate average stability by using Boltzmann distribution. The stability scores ($\Delta\Delta G_s$) of the structures refined by energy minimization were obtained through the stability scoring function of the Protein Design application and are indicated below the structural model.

PBMCs. In contrast, the replication efficiency of MN4/LSDQ was markedly enhanced in *TRIM5*α homozygous CyM PBMCs relative to that of MN4Rh-3 (Fig. 5A). Similar results were obtained with RhM PBMCs. MN4Rh-3 exhibited growth kinetics comparable to those of MN4/LSDQ in *TRIM5*α/*TRIM5CypA* heterozygous RhM PBMCs (Fig. 5B). In *TRIM5*α homozygous RhM PBMCs, MN5/LSDQ replicated much more efficiently than MN5Rh-3 (Fig. 5C). CXCR4-tropic HIV-1mt clones (MN4 series) were found to exhibit a higher growth ability than CCR5-tropic HIV-1mt clones (MN5 series) in both M1.3S cells and macaque PBMCs (Fig. 2D and 5B and C) and were therefore used for experiments thereafter. In sum, the replication potential of TRIM5α-resistant HIV-1mt clones (MN4/LSDQ and MN5/LSDQ) markedly increased in *TRIM5*α homozygous PBMCs but was similar to that of TRIM5CypA-resistant/TRIM5α-sensitive clones (MN4Rh-3 and MN5Rh-3) in *TRIM5*α/*TRIM5CypA* heterozygous PBMCs. These results suggest that M94L/R98S/G114Q mutations in MN4Rh-3 CA largely contribute to the acquisition of TRIM5α resistance.

HIV-1 Vpu gains the ability to specifically counteract macaque tetherin by replacing its TM domain with the corresponding region of SIVgsn166 Vpu. Tetherin as well as TRIM5 proteins are important anti-HIV-1 factors in macaque cells (4, 8, 10), but the HIV-1mt clones constructed so far do not display macaque tetherin antagonism due to Vpu derived from HIV-1_{NL4-3}. It has been shown that Vpu from SIVmon/mus/gsn can antagonize macaque tetherin but not human tetherin (26). To confer the ability to counteract macaque tetherin on HIV-1mt clones, we modified the *vpu* gene. The sequence of the cytoplasmic domain of HIV-1 Vpu partially overlaps the 5′-end sequence of Env, and the TM domain of Vpu is a key region for species-specific tetherin antagonism (22). Thus, we constructed Vpu clones that contain SIVmon/mus/gsn TM and HIV-1mt cytoplasmic domains (Fig. 6A). First, RhM tetherin antagonism of various Vpu clones was analyzed by Vpu *trans*-complementation assays for virion release (Fig. 6B). 293T cells were cotransfected with a *vpu*-deficient HIV-1mt clone (MN4Rh-3-ΔU), an RhM tetherin expression vector (pCIneo-RhM tetherin), and various Vpu constructs, and virion production from cells on day 2 posttransfection was measured. While MN4Rh-3-ΔU released progeny virions efficiently upon transfection without RhM tetherin expression, its virion production was significantly inhibited in the presence of RhM tetherin. Although this reduction was not rescued by HIV-1_{NL4-3} Vpu, SIVmon/mus/gsn Vpu restored it to some extent, consistent with a previous report (26). Of the SIV/HIV-1 chimeric Vpu proteins, gsnTM-Vpu appeared to be somewhat better than the others and was therefore used thereafter.

Next, we examined the ability of HIV-1_{NL4-3} Vpu and gsnTM-Vpu to downregulate cell surface CD4 and tetherin (Fig. 6C). MAGI, LLC-MK2, and HEp2 cells were used for analysis of CD4,

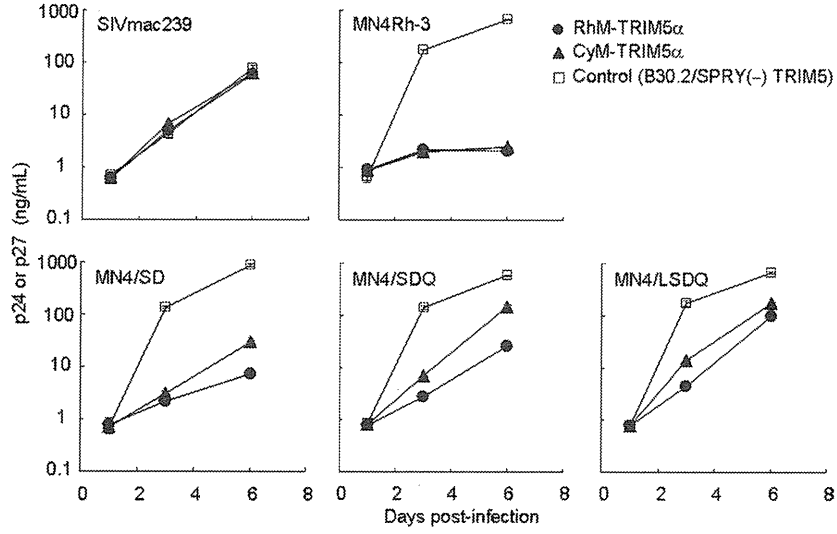

FIG 4 Susceptibility of SIVmac239 and various HIV-1mt clones to macaque TRIM5α. Human MT4 cells (10^5) were infected with recombinant SeV expressing RhM-TRIM5α (*TRIM5*^{TFP}), CyM-TRIM5α (*TRIM5*^{Q}), or B30.2/SPRY(−) TRIM5. Nine hours after infection, cells were superinfected with 20 ng (Gag-p24) of various HIV-1mt clones or 20 ng (Gag-p27) of SIVmac239. Virus replication was monitored by the amount of Gag-p24 from HIV-1mt clones or Gag-p27 from SIVmac239 in the culture supernatants. Error bars show actual fluctuations between duplicate samples. Representative data from two independent experiments are shown.

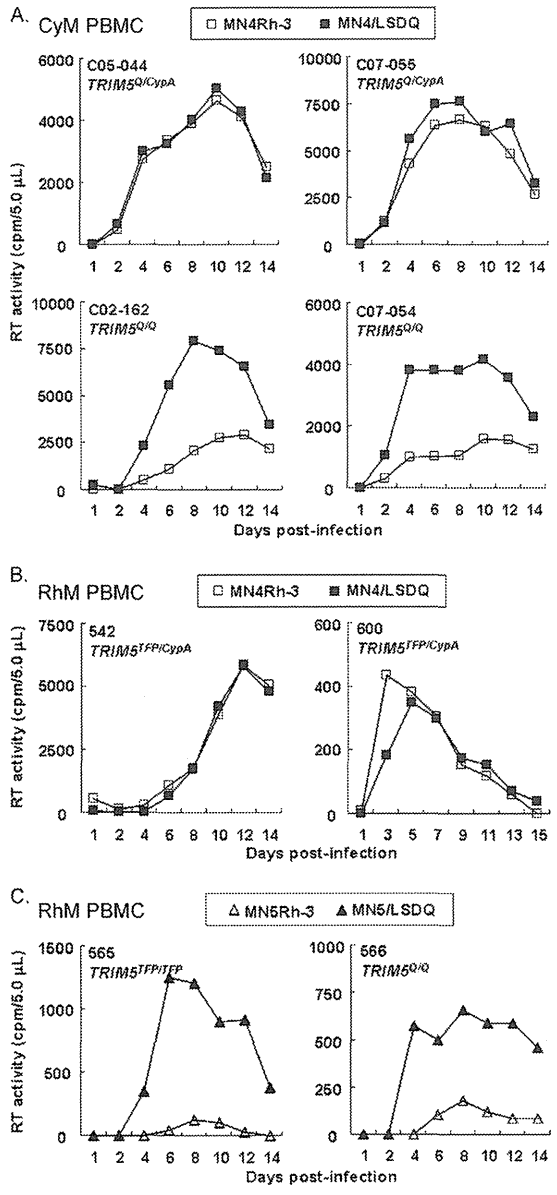

FIG 5 Growth kinetics of HIV-1mt clones with a distinct CA in macaque PBMCs. (A) Infection of PBMCs from four *TRIM5α/TRIM5CypA* heterozygous or *TRIM5α* homozygous CyM individuals. (B and C) Infection of PBMCs from four RhM individuals with different *TRIM5* alleles. For infection, input viruses were prepared from 293T cells transfected with the proviral clones indicated, and equal amounts (2.5×10^6 RT units) were used to spin infect PBMCs (2×10^6 cells). Virus replication was monitored by RT activity released into the culture supernatants. Monkey identification numbers are indicated in each panel.

RhM tetherin, and human tetherin, respectively. Cells were transfected with Vpu-green fluorescent protein (GFP) bicistronic expression plasmids and subjected to flow cytometry analysis on day 2 posttransfection. While both HIV-1_{NL4-3} Vpu and gsnTM-Vpu significantly decreased cell surface CD4 levels, the RhM tetherin level was reduced by gsnTM-Vpu but not by HIV-1_{NL4-3} Vpu. Similar results were obtained for MK.P3(F) cells expressing endogenous CyM tetherin (data not shown). In contrast, HIV-1_{NL4-3} Vpu but not gsnTM-Vpu downmodulated cell surface human tetherin. These results show that the transfer of the SIVgsn166 Vpu TM domain to HIV-1 Vpu is sufficient to confer the ability to specifically antagonize macaque tetherin on viruses.

gsnTM-Vpu in the context of proviral genome functions in macaque cells. To ask if gsnTM-Vpu is functional in the proviral context, we generated an HIV-1mt clone encoding gsnTM-Vpu (MN4/LSDQgtu) (Fig. 1 and 7A). Interestingly, it has been shown that Vpu of HIV-1 composed of HIV-1_{DH12} TM and HIV-1_{NL4-3} cytoplasmic domains counteracts macaque tetherin (22). We thus constructed another HIV-1mt clone, MN4/LSDQdtu, that has chimeric Vpu, as described above (Fig. 7A).

To examine the species-specific tetherin antagonism of these proviral clones, we carried out virion release assays in the presence of RhM or human tetherin (Fig. 7B). Using SIVmac239 Nef as a control antagonist against macaque tetherin (52, 53), the anti-macaque tetherin activities of MN4/LSDQ, MN4/LSDQdtu, and MN4/LSDQgtu were comparatively analyzed. As described above, SIVmac239 Nef exhibited the ability to specifically antagonize macaque tetherin. As expected, virion production of MN4/LSDQ and its *vpu*-deficient clone was similarly restricted in the presence of RhM tetherin, and MN4/LSDQ displayed a higher level of virion production than that of its *vpu*-deficient clone in the presence of human tetherin, indicating its specific antagonism to human tetherin. Also, as expected from a previous report (22), MN4/LSDQdtu showed both RhM and human tetherin antagonism, although its anti-RhM tetherin activity was relatively low. Strikingly, virion production levels of MN4/LSDQgtu in the presence of RhM/human tetherin were similar to those of SIVmac239. This indicates that MN4/LSDQgtu has specifically strong anti-RhM tetherin activity, as is the case for SIVmac239. To see if various Vpu proteins function during viral replication in macaque cells, we determined the growth properties of various HIV-1mt clones carrying distinct Vpu proteins. Although the effect of *vpu* deletion is virologically small, *vpu*-deficient viruses are readily distinguishable from the parental wild-type virus by comparative kinetic analysis of viral growth (22, 29). As shown in Fig. 7C, while MN4/LSDQ and MN4/LSDQdtu exhibited growth kinetics similar to those of their respective *vpu*-deficient clones, *vpu*-deficient MN4/LSDQgtu grew significantly more poorly than its parental virus. Taken together, it can be concluded that MN4/LSDQgtu Vpu but not MN4/LSDQ Vpu functions during viral replication in M1.3S cells. However, the functionality of MN4/LSDQdtu Vpu in macaque cells was not clear in the viral growth kinetics here. Although there are some possible explanations, the relatively low anti-RhM tetherin activity of MN4/LSDQdtu (see the results in Fig. 7B) could account for this observation.

Although the tertiary structure of the HIV-1 Vpu TM domain has been determined by NMR (38), the structure of the TM domain from SIV Vpu has not been solved to date. To investigate how replacement of the Vpu TM domain could lead to changes in TM structure, we constructed structural models of Vpu TM domains of MN4/LSDQ, MN4/LSDQdtu, and MN4/LSDQgtu (Fig. 7D). This modeling study revealed that the types of amino acid residues corresponding to the crucial residues (54) in HIV-1 Vpu for binding with human tetherin are similar between MN4/LSDQ and MN4/LSDQdtu, whereas they are often different in MN4/LSDQgtu. In addition, their steric locations in the helices are also similar between MN4/LSDQ and MN4/LSDQdtu, whereas they are very different in MN4/LSDQgtu. Finally, angles between the

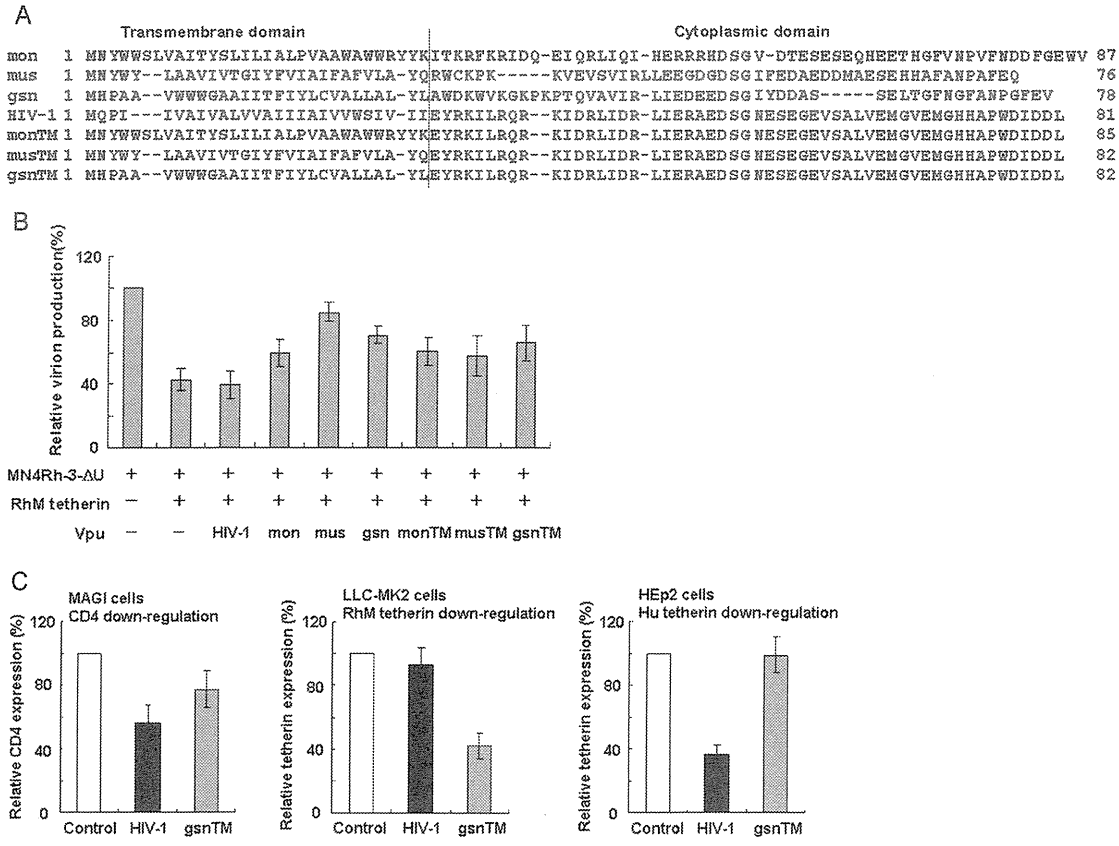

FIG 6 Generation of SIV/HIV-1 chimeric Vpu proteins resistant to macaque tetherin. (A) Amino acid sequences of various Vpu proteins. Alignments of the sequences and the boundary between TM/cytoplasmic domains are shown based on previously reported information (26). mon, SIVmonCML1 (GenBank accession number AY340701); mus, SIVmus1085 (GenBank accession number AY340700); gsn, SIVgsn166 (GenBank accession number AF468659); HIV-1, NL4-3 (32). HIV-1mt clones (MN4 series) have *vpu* genes identical to that of NL4-3. monTM-, musTM-, and gsnTM-Vpu were constructed by fusing each TM domain of SIVmon/mus/gsn Vpu with the cytoplasmic domain of HIV-1_{NL4-3} Vpu. (B) RhM tetherin antagonism by various Vpu proteins. 293T cells were cotransfected with a *vpu*-deficient proviral clone (MN4Rh-3-ΔU), pCIneo-RhM tetherin, and various pSG-VpucFLAG constructs. On day 2 posttransfection, virion production in the culture supernatants was determined by RT assays. Virion production levels relative to that of MN4Rh-3-ΔU in the absence of RhM tetherin were calculated, and mean values of three independent experiments are shown with the standard deviations. (C) Downregulation of cell surface CD4 and tetherin by HIV-1_{NL4-3} Vpu or gsnTM-Vpu. MAGI, LLC-MK2, and HEp2 cells were used to determine the downregulation of CD4, RhM tetherin, and human (Hu) tetherin by Vpu, respectively. Cells were transfected with the pIRES-hrGFP (control), pIRES-HIV-1 Vpu-hrGFP, or pIRES-gsnTM-Vpu-hrGFP construct. On day 2 posttransfection, cells were stained for cell surface CD4 or tetherin and analyzed by two-color flow cytometry. Values presented are CD4 or tetherin fluorescence intensities of GFP-positive cells relative to that of the control. Mean values ± standard deviations of three independent experiments are shown.

central lines of the helices are similar between MN4/LSDQ and MN4/LSDQdtu, whereas they are different in MN4/LSDQgtu. These results suggest the possibility that the structural properties of the tetherin interaction surface of the MN4/LSDQgtu Vpu TM domain are very different from those of the Vpu TM domains of MN4/LSDQ and MN4/LSDQdtu. Further studies are necessary to verify this issue.

RhM APOBEC3-, TRIM5α-, and tetherin-resistant HIV-1mt clone MN4/LSDQgtu replicates comparably to SIVmac239 in RhM PBMCs. Here we constructed distinct HIV-1mt clones with respect to their resistance to RhM TRIM5α and tetherin: TRIM5α- and tetherin-susceptible MN4Rh-3, TRIM5α-resistant but tetherin-susceptible MN4/LSDQ, and TRIM5α- and tetherin-resistant MN4/LSDQgtu. Of note, all these clones are RhM APOBEC3 resistant (see Fig. 1 for their genomes). To investigate the effect of the increased resistance to these macaque restriction factors, various viruses were examined for their growth potential in PBMCs from four *TRIM5α* homozygous RhM individuals. As shown in Fig. 8, SIVmac239, a comparative standard virus in macaque cells, replicated constantly in all PBMC preparations. The growth potentials in the RhM PBMCs of the HIV-1mt clones tested markedly and stably differed. As a likely result of RhM TRIM5α-resistant Gag-CA, MN4/LSDQ replicated much more efficiently than MN4Rh-3. By virtue of RhM tetherin-resistant Vpu, MN4/LSDQgtu grew significantly better than MN4/LSDQ. Essentially the same results for HIV-1mt growth kinetics were obtained in M1.3S cells. The M1.3S cell line and macaque PBMCs always responded similarly to various SIVs/HIVs (our unpublished observations). Moreover, by comparing the peak day of viral growth kinetics and the peak level itself, MN4/LSDQgtu was shown here to have the ability to replicate comparably to SIVmac239 in RhM PBMCs, except for one preparation (from monkey 565) (Fig. 8). The results show that the increased resistance to macaque restriction factors correlates well with the enhanced viral growth potential. In sum, MN4/LSDQgtu, which exhibits resistance to known major restriction factors (APOBEC3, TRIM5, and tetherin

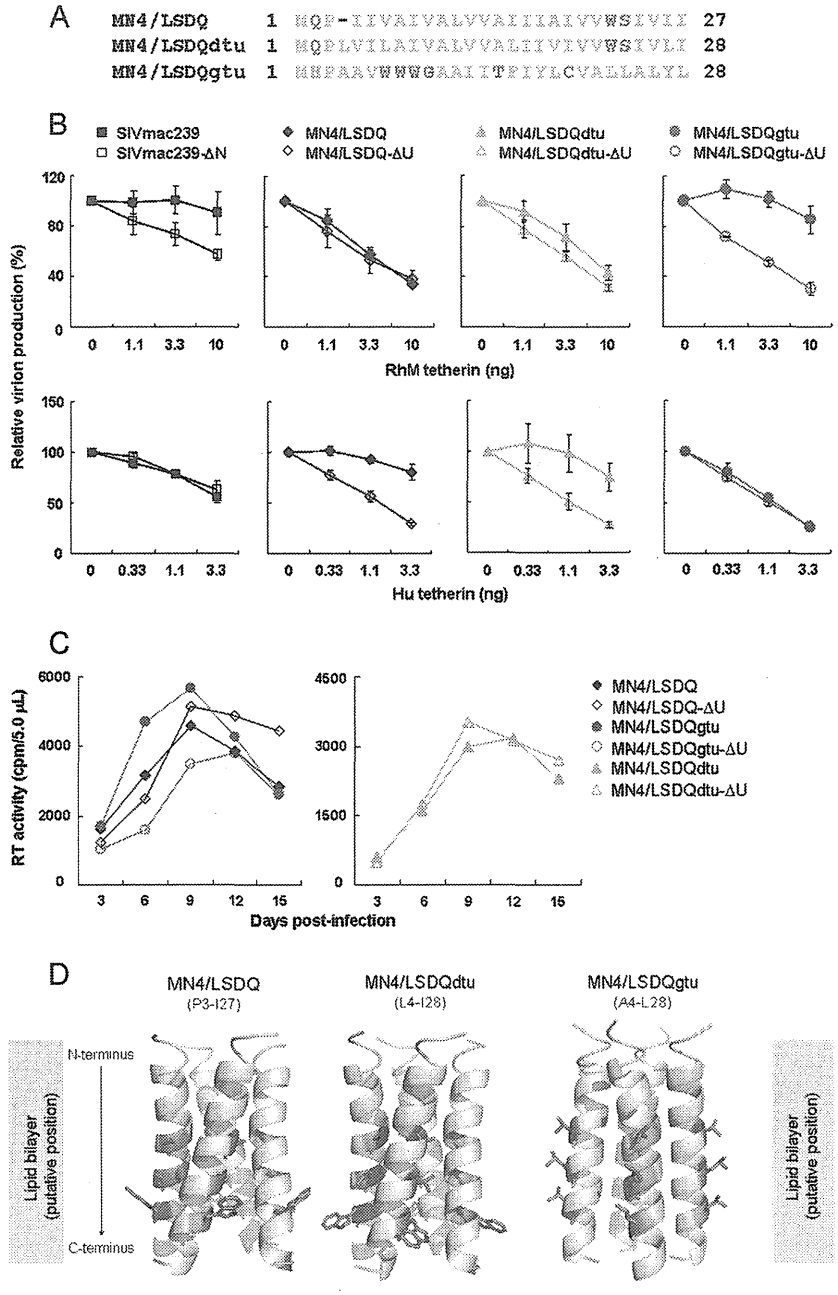

FIG 7 Effects of various Vpu proteins carrying a different TM domain on tetherin antagonism and HIV-1mt replication in macaque cells. (A) Alignment of amino acid sequences of the Vpu TM domain in each HIV-1mt clone. MN4/LSDQ, MN4/LSDQdtu, and MN4/LSDQgtu encode the Vpu TM domain derived from HIV-1_{NL4-3} (32), HIV-1_{DH12} (22), and SIVgsn166 (GenBank accession number AF468659), respectively. (B) Species-specific tetherin antagonism by SIVmac239 and various HIV-1mt clones carrying different Vpu proteins. SIVmac239 (MA239N) and its *nef*-deficient clone (MA239N-ΔN) were used as positive controls for RhM tetherin resistance. 293T cells were cotransfected with proviral clones and the indicated amounts of the pCIneo-RhM tetherin or pCIneo-Human tetherin expression vector. On day 2 posttransfection, virion production was determined by RT activity released into the culture supernatants. Values are presented as RT activity of each sample relative to that of each proviral clone without tetherin expression. Mean values ± standard deviations of three independent experiments are shown. ΔU, *vpu* deficient; Hu, human. (C) Growth kinetics of various HIV-1mt clones and their *vpu*-deficient clones in M1.3S cells. Viruses were prepared from 293T cells transfected with the indicated proviral clones, and equal amounts (5×10^5 RT units) were inoculated into M1.3S cells (2×10^5 cells). Virus replication was monitored by RT activity released into the culture supernatants. Representative data from three independent experiments are shown. (D) Structural modeling of Vpu TM domains of MN4/LSDQ, MN4/LSDQdtu, and MN4/LSDQgtu. Predicted models are shown in a ribbon representation. Amino acid residues corresponding to the residues in HIV-1 Vpu crucial for binding with human tetherin (54) are highlighted in a red stick representation. Crucial residues in Vpu TM domains of MN4/LSDQ, MN4/LSDQdtu, and MN4/LSDQgtu are A14/A18/W22, A15/V19/W23, and T15/L19/L23, respectively. TM regions analyzed (see panel A for amino acid sequences) are indicated in parentheses.

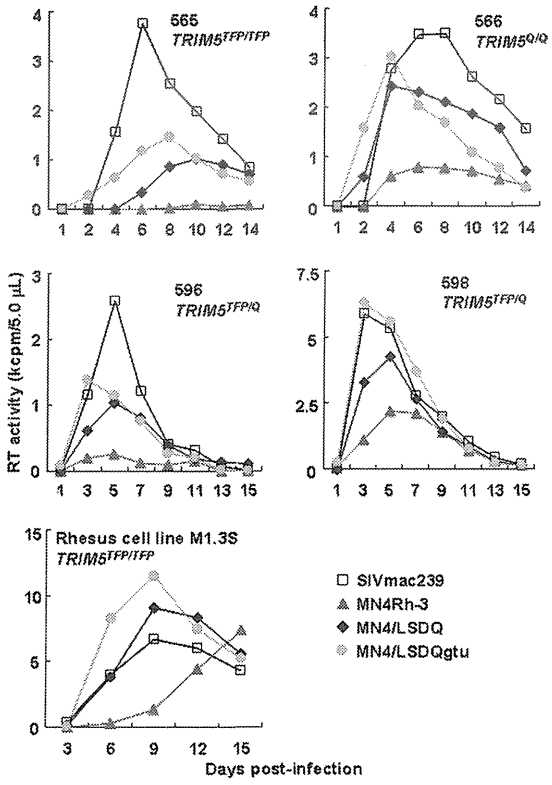

FIG 8 Growth kinetics of SIVmac239 and various HIV-1mt clones in *TRIM5α* homozygous RhM PBMCs. PBMCs were prepared from four RhM individuals with the different *TRIM5* alleles indicated. Viruses were prepared from 293T cells transfected with the indicated proviral clones, and equal amounts (2.5×10^6 RT units) were used to spin infect PBMCs (2×10^6 cells). As a control experiment, rhesus M1.3S cells (2×10^5) were infected with equal amounts of viruses (5×10^5 RT units). Virus replication was monitored by RT activity released into the culture supernatants. Monkey identification numbers are indicated in each panel.

proteins), is the best HIV-1mt clone generated so far, replicating with an efficiency similar to that of SIVmac239 in RhM cells.

DISCUSSION

In this study, we generated a novel HIV-1mt clone, designated MN4/LSDQgtu, that exhibits resistance to RhM TRIM5α and tetherin in addition to APOBEC3 proteins (Fig. 1). By sequence homology- and structure-guided CA mutagenesis and by screening the multicycle growth potential of CA mutant viruses in M1.3S cells, we successfully obtained viruses with enhanced replication efficiency in macaque cells as well as increased macaque TRIM5α resistance (Fig. 2 to 5). The transfer of the TM domain of SIVgsn166 Vpu into the corresponding region of HIV-1mt Vpu conferred the ability to specifically counteract macaque tetherin on the virus (Fig. 6 and 7). Furthermore, the increased resistance to both RhM TRIM5α and tetherin contributed to the viral growth enhancement in RhM PBMCs (Fig. 8).

During the preparation of this paper, McCarthy et al. reported several key residues in SIVmac239 CA involved in the interaction with RhM TRIM5α by genetic and structural analysis (55). Interestingly, the HIV-1mt CA amino acid residues identified in this study as being the elements responsible for the increased resistance to RhM TRIM5α (M94L/R98S/Q110D/G114Q) were included in those residues. McCarthy et al. reported that H4/5L and helix 6 of SIVmac239 CA also affect TRIM5α sensitivity (55). In the construction process for our HIV-1mt clones, we found that the CA elements involved in the interaction with RhM TRIM5α are the CypA-binding loop within H4/5L, H6/7L, M94L/R98S within H4/5L, and Q110D/G114Q in helix 6 (18–20, 56; this study). Of the substitutions identified in this study, R98S was the primary residue to increase TRIM5α resistance and improve viral growth in macaque cells. It was also shown that the TRIM5α (*TRIM5*^{TFP})-susceptible SIVsmE543-3 clone acquires an adaptive R97S change in CA (corresponding to R98S in MN4Rh-3 CA) to evade TRIM5α (*TRIM5*^{TFP}) restriction during viral replication in RhM individuals (40). In TRIM5α-sensitive CA, R98S may be a key residue contributing to the evasion of TRIM5α restriction. Together, these results suggest that CA elements critical for recognition by TRIM5α may be conserved among primate lentiviruses. The RhM TRIM5α-resistant HIV-1 CA constructed in this study would be useful to define how TRIM5α recognizes CA. On the other hand, MN4/LSDQ appeared not to evade TRIM5α restriction completely, as SIVmac239 did (Fig. 4). In this regard, since it has been shown that the N-terminal β-hairpin domain in the retroviral CA contributes to circumventing TRIM5α (36, 55, 57), we constructed various HIV-1mt clones carrying mutations in the domain (Table 1). However, except for the L6I substitution, none of the clones were infectious (Table 1). A further CA modification(s) may be necessary for complete evasion of TRIM5α restriction.

Accumulating evidence has shown that tetherin is an important cellular restriction factor that affects the replication, adaptation, and evolution of primate immunodeficiency viruses (4, 26). Its negative effect on viral replication is certainly observed in cultured cell lines and primary cells but is not so evident relative to those of APOBEC3 and TRIM5 proteins (10). Also, in the present study, RhM tetherin-resistant Vpu significantly contributed to viral growth enhancement but not as much as TRIM5α-resistant CA (Fig. 7 and 8). However, tetherin has been suggested to play an important effector role in antiretroviral activity induced by alpha interferon (58–60). Also, it has been shown that the pathogenic revertant virus from nonpathogenic *nef*-deficient virus acquires tetherin antagonism by adaptive mutations in the gp41 subunit of Env (61). Therefore, the ability of HIV-1mt clones to antagonize RhM tetherin may be very important for optimal replication and pathogenesis in RhM individuals. In this regard, it has been described that naturally occurring polymorphisms in RhM tetherin sequences are present (30, 31, 61). Although whether these variations have some appreciable effects on viral replication *in vitro* is undetermined, the relationship between tetherin polymorphisms and the viral replication level *in vivo* (animals)/viral pathogenic activity *in vivo* may be a major issue to address and remains to be extensively analyzed. It would be intriguing to elucidate how the viral accessory protein Vpu *in vitro* is associated with the *in vivo* replicative and pathogenic properties of HIV-1 (22).

We constructed an MN4/LSDQgtu clone resistant to the known major restriction factors (APOBEC3, TRIM5, and tetherin proteins) in RhM cells. The growth potential of MN4/LSDQgtu was similar to that of SIVmac239 in most RhM PBMC preparations (Fig. 8). It was shown previously that the *in vivo* replication of SIV is predictable from the virus susceptibility of PBMCs (62, 63). Also, in a series of our studies, the better our HIV-1mt clones grew in PBMCs, the better they grew in the monkeys (20, 24, 64).

Thus, it is expected that MN4/LSDQgtu will grow much better in RhM individuals, at least in the early infection phase, than the other HIV-1mt clones constructed. As reported previously, the replication of HIV-1 derivatives in infected macaques was eventually controlled, and no disease was induced in the animals (16, 20, 21, 24, 64). It has been suggested that the replication ability of primate lentiviruses in unusual hosts is more severely affected, via an interferon-induced antiviral state mediated by unidentified species-specific factors, than that in natural hosts (23). Moreover, there are the other significant issues to be considered, such as viral coreceptor tropism (CXCR4 versus CCR5), the diversity in viral growth properties (HIV-1 versus SIVmac), and the difference in host immune responses (human versus RhM) (9, 65–67). Most importantly, CCR5-tropic but not CXCR4-tropic clones have been found to be appropriate as input viruses to experimentally infect RhMs for various HIV-1 model studies *in vivo* (65–67). Although MN4/LSDQgtu is a CXCR4-tropic virus, it has clear potential for the establishment of a model system. MN4/LSDQgtu can be changed to a pathogenic CCR5-tropic virus through *in vitro* and *in vivo* approaches, as well documented by previous SHIV studies (68–70). It is also possible to generate entirely new CCR5-tropic HIV-1mt clones other than MN4/LSDQgtu derivatives on the basis of the key findings for Gag-CA and Vpu-TM in this study.

Our study here describes the generation and characterization of a novel HIV-1 derivative minimally chimeric with SIVs. Several infection model systems using distinct viruses and nonhuman primates are now available. It is important to define common and unique characteristics of each virus-host interaction based on the results obtained from various experimental approaches, including SIV/natural host and SIVmac/RhM, SHIV/RhM, and HIV-1mt/RhM infection systems. Such efforts would shed light on a better understanding of HIV-1/human infection and HIV-1 pathogenesis.

ACKNOWLEDGMENTS

This study was supported in part by a grant from the Ministry of Health, Labor and Welfare of Japan (Research on HIV/AIDS project no. H23-003).

We thank Kazuko Yoshida for editorial assistance.

We declare that no competing interests exist.

REFERENCES

1. **Kirchhoff F.** 2010. Immune evasion and counteraction of restriction factors by HIV-1 and other primate lentiviruses. Cell Host Microbe **8**:55–67.
2. **Sharp PM, Hahn BH.** 2011. Origins of HIV and the AIDS pandemic. Cold Spring Harb. Perspect. Med. **1**:a006841. doi:10.1101/cshperspect.a006841.
3. **Shibata R, Sakai H, Kawamura M, Tokunaga K, Adachi A.** 1995. Early replication block of human immunodeficiency virus type 1 in monkey cells. J. Gen. Virol. **76**:2723–2730.
4. **Blanco-Melo D, Venkatesh S, Bieniasz PD.** 2012. Intrinsic cellular defenses against human immunodeficiency viruses. Immunity **37**:399–411.
5. **Harris RS, Hultquist JF, Evans DT.** 2012. The restriction factors of human immunodeficiency virus. J. Biol. Chem. **287**:40875–40883.
6. **Malim MH, Bieniasz PD.** 2012. HIV restriction factors and mechanisms of evasion. Cold Spring Harb. Perspect. Med. **2**:a006940. doi:10.1101/cshperspect.a006940.
7. **Hatziioannou T, Evans DT.** 2012. Animal models for HIV/AIDS research. Nat. Rev. Microbiol. **10**:852–867.
8. **Nomaguchi M, Doi N, Fujiwara S, Adachi A.** 2011. Macaque-tropic HIV-1 derivatives: a novel experimental approach to understand viral replication and evolution *in vivo*, p 325–348. *In* Chang T.Y.-L. (ed), HIV-host interactions. InTech, Rijeka, Croatia. http://www.intechopen.com/books/hiv-host-interactions/macaque-tropic-hiv-1-derivatives-a-novel-experimental-approach-to-understand-viral-replication-and-e.
9. **Shedlock DJ, Silvestri G, Weiner DB.** 2009. Monkeying around with HIV vaccines: using rhesus macaques to define 'gatekeepers' for clinical trials. Nat. Rev. Immunol. **9**:717–728.
10. **Nomaguchi M, Doi N, Matsumoto Y, Sakai Y, Fujiwara S, Adachi A.** 2012. Species tropism of HIV-1 modulated by viral accessory proteins. Front. Microbiol. **3**:267. doi:10.3389/fmicb.2012.00267.
11. **Holmes RK, Malim MH, Bishop KN.** 2007. APOBEC-mediated viral restriction: not simply editing? Trends Biochem. Sci. **32**:118–128.
12. **Malim MH, Emerman M.** 2008. HIV-1 accessory proteins—ensuring viral survival in a hostile environment. Cell Host Microbe **3**:388–398.
13. **Grütter MG, Luban J.** 2012. TRIM5 structure, HIV-1 capsid recognition, and innate immune signaling. Curr. Opin. Virol. **2**:142–150.
14. **Nakayama EE, Shioda T.** 2010. Anti-retroviral activity of TRIM5 alpha. Rev. Med. Virol. **20**:77–92.
15. **Douglas JL, Gustin JK, Viswanathan K, Mansouri M, Moses AV, Früh K.** 2010. The great escape: viral strategies to counter BST-2/tetherin. PLoS Pathog. **6**:e1000913. doi:10.1371/journal.ppat.1000913.
16. **Hatziioannou T, Ambrose Z, Chung NP, Piatak M, Jr, Yuan F, Trubey CM, Coalter V, Kiser R, Schneider D, Smedley J, Pung R, Gathuka M, Estes JD, Veazey RS, KewalRamani VN, Lifson JD, Bieniasz PD.** 2009. A macaque model of HIV-1 infection. Proc. Natl. Acad. Sci. U. S. A. **106**:4425–4429.
17. **Hatziioannou T, Princiotta M, Piatak M, Jr, Yuan F, Zhang F, Lifson JD, Bieniasz PD.** 2006. Generation of simian-tropic HIV-1 by restriction factor evasion. Science **314**:95. doi:10.1126/science.1130994.
18. **Kamada K, Igarashi T, Martin MA, Khamsri B, Hatcho K, Yamashita T, Fujita M, Uchiyama T, Adachi A.** 2006. Generation of HIV-1 derivatives that productively infect macaque monkey lymphoid cells. Proc. Natl. Acad. Sci. U. S. A. **103**:16959–16964.
19. **Nomaguchi M, Yokoyama M, Kono K, Nakayama EE, Shioda T, Saito A, Akari H, Yasutomi Y, Matano T, Sato H, Adachi A.** 2013. Gag-CA Q110D mutation elicits TRIM5-independent enhancement of HIV-1mt replication in macaque cells. Microbes Infect. **15**:56–65.
20. **Saito A, Nomaguchi M, Iijima S, Kuroishi A, Yoshida T, Lee YJ, Hayakawa T, Kono K, Nakayama EE, Shioda T, Yasutomi Y, Adachi A, Matano T, Akari H.** 2011. Improved capacity of a monkey-tropic HIV-1 derivative to replicate in cynomolgus monkeys with minimal modifications. Microbes Infect. **13**:58–64.
21. **Thippeshappa R, Polacino P, Yu Kimata MT, Siwak EB, Anderson D, Wang W, Sherwood L, Arora R, Wen M, Zhou P, Hu SL, Kimata JT.** 2011. Vif substitution enables persistent infection of pig-tailed macaques by human immunodeficiency virus type 1. J. Virol. **85**:3767–3779.
22. **Shingai M, Yoshida T, Martin MA, Strebel K.** 2011. Some human immunodeficiency virus type 1 Vpu proteins are able to antagonize macaque BST-2 *in vitro* and *in vivo*: Vpu-negative simian-human immunodeficiency viruses are attenuated *in vivo*. J. Virol. **85**:9708–9715.
23. **Bitzegeio J, Sampias M, Bieniasz PD, Hatziioannou T.** 2013. Adaptation to the interferon-induced antiviral state by human and simian immunodeficiency viruses. J. Virol. **87**:3549–3560.
24. **Saito A, Nomaguchi M, Kono K, Iwatani Y, Yokoyama M, Yasutomi Y, Sato H, Shioda T, Sugiura W, Matano T, Adachi A, Nakayama E, Akari H.** 2013. *TRIM5* genotypes in cynomolgus monkeys primarily influence inter-individual diversity in susceptibility to monkey-tropic human immunodeficiency virus type 1. J. Gen. Virol. **94**:1318–1324.
25. **Doi N, Fujiwara S, Adachi A, Nomaguchi M.** 2011. Rhesus M1.3S cells suitable for biological evaluation of macaque-tropic HIV/SIV clones. Front. Microbiol. **2**:115. doi:10.3389/fmicb.2011.00115.
26. **Sauter D, Schindler M, Specht A, Landford WN, Münch J, Kim KA, Votteler J, Schubert U, Bibollet-Ruche F, Keele BF, Takehisa J, Ogando Y, Ochsenbauer C, Kappes JC, Ayouba A, Peeters M, Learn GH, Shaw G, Sharp PM, Bieniasz P, Hahn BH, Hatziioannou T, Kirchhoff F.** 2009. Tetherin-driven adaptation of Vpu and Nef function and the evolution of pandemic and nonpandemic HIV-1 strains. Cell Host Microbe **6**:409–421.
27. **Lebkowski JS, Clancy S, Calos MP.** 1985. Simian virus 40 replication in adenovirus-transformed human cells antagonizes gene expression. Nature **317**:169–171.
28. **Kimpton J, Emerman M.** 1992. Detection of replication-competent and pseudotyped human immunodeficiency virus with a sensitive cell line on the basis of activation of an integrated beta-galactosidase gene. J. Virol. **66**:2232–2239.
29. **Nomaguchi M, Doi N, Fujiwara S, Fujita M, Adachi A.** 2010. Site-

directed mutagenesis of HIV-1 *vpu* gene demonstrates two clusters of replication-defective mutants with distinct ability to down-modulate cell surface CD4 and tetherin. Front. Microbiol. 1:116. doi:10.3389/fmicb.2010.00116.
30. McNatt MW, Zang T, Hatziioannou T, Bartlett M, Fofana IB, Johnson WE, Neil SJ, Bieniasz PD. 2009. Species-specific activity of HIV-1 Vpu and positive selection of tetherin transmembrane domain variants. PLoS Pathog. 5:e1000300. doi:10.1371/journal.ppat.1000300.
31. Yoshida T, Kao S, Strebel K. 2011. Identification of residues in the BST-2 TM domain important for antagonism by HIV-1 Vpu using a gain-of-function approach. Front. Microbiol. 2:35. doi:10.3389/fmicb.2011.00035.
32. Adachi A, Gendelman HE, Koenig S, Folks T, Willey R, Rabson A, Martin MA. 1986. Production of acquired immunodeficiency syndrome-associated retrovirus in human and nonhuman cells transfected with an infectious molecular clone. J. Virol. 59:284–291.
33. Willey RL, Smith DH, Lasky LA, Theodore TS, Earl PL, Moss B, Capon DJ, Martin MA. 1988. In vitro mutagenesis identifies a region within the envelope gene of the human immunodeficiency virus that is critical for infectivity. J. Virol. 62:139–147.
34. O'Doherty U, Swiggard WJ, Malim MH. 2000. Human immunodeficiency virus type 1 spinoculation enhances infection through virus binding. J. Virol. 74:10074–10080.
35. Wilson SJ, Webb BL, Ylinen LM, Verschoor E, Heeney JL, Towers GJ. 2008. Independent evolution of an antiviral TRIMCyp in rhesus macaques. Proc. Natl. Acad. Sci. U. S. A. 105:3557–3562.
36. Kono K, Song H, Yokoyama M, Sato H, Shioda T, Nakayama EE. 2010. Multiple sites in the N-terminal half of simian immunodeficiency virus capsid protein contribute to evasion from rhesus monkey TRIM5α-mediated restriction. Retrovirology 7:72. doi:10.1186/1742-4690-7-72.
37. Howard BR, Vajdos FF, Li S, Sundquist WI, Hill CP. 2003. Structural insights into the catalytic mechanism of cyclophilin A. Nat. Struct. Biol. 10:475–481.
38. Park SH, Mrse AA, Nevzorov AA, Mesleh MF, Oblatt-Montal M, Montal M, Opella SJ. 2003. Three-dimensional structure of the channel-forming trans-membrane domain of virus protein "u" (Vpu) from HIV-1. J. Mol. Biol. 333:409–424.
39. Leaver-Fay A, Tyka M, Lewis SM, Lange OF, Thompson J, Jacak R, Kaufman K, Renfrew PD, Smith CA, Sheffler W, Davis IW, Cooper S, Treuille A, Mandell DJ, Richter F, Ban YE, Fleishman SJ, Corn JE, Kim DE, Lyskov S, Berrondo M, Mentzer S, Popović Z, Havranek JJ, Karanicolas J, Das R, Meiler J, Kortemme T, Gray JJ, Kuhlman B, Baker D, Bradley P. 2011. ROSETTA3: an object-oriented software suite for the simulation and design of macromolecules. Methods Enzymol. 487:545–574.
40. Kirmaier A, Wu F, Newman RM, Hall LR, Morgan JS, O'Connor S, Marx PA, Meythaler M, Goldstein S, Buckler-White A, Kaur A, Hirsch VM, Johnson WE. 2010. *TRIM5* suppresses cross-species transmission of a primate immunodeficiency virus and selects for emergence of resistant variants in the new species. PLoS Biol. 8:e1000462. doi:10.1371/journal.pbio.1000462.
41. Newman RM, Hall L, Connole M, Chen GL, Sato S, Yuste E, Diehl W, Hunter E, Kaur A, Miller GM, Johnson WE. 2006. Balancing selection and the evolution of functional polymorphism in Old World monkey TRIM5alpha. Proc. Natl. Acad. Sci. U. S. A. 103:19134–19139.
42. Price AJ, Marzetta F, Lammers M, Ylinen LM, Schaller T, Wilson SJ, Towers GJ, James LC. 2009. Active site remodeling switches HIV specificity of antiretroviral TRIMCyp. Nat. Struct. Mol. Biol. 16:1036–1042.
43. Ylinen LM, Price AJ, Rasaiyaah J, Hué S, Rose NJ, Marzetta F, James LC, Towers GJ. 2010. Conformational adaptation of Asian macaque TRIMCyp directs lineage specific antiviral activity. PLoS Pathog. 6:e1001062. doi:10.1371/journal.ppat.1001062.
44. Fassati A. 2012. Multiple roles of the capsid protein in the early steps of HIV-1 infection. Virus Res. 170:15–24.
45. Ganser-Pornillos BK, Yeager M, Sundquist WI. 2008. The structural biology of HIV assembly. Curr. Opin. Struct. Biol. 18:203–217.
46. Miyamoto T, Yokoyama M, Kono K, Shioda T, Sato H, Nakayama EE. 2011. A single amino acid of human immunodeficiency virus type 2 capsid protein affects conformation of two external loops and viral sensitivity to TRIM5α. PLoS One 6:e22779. doi:10.1371/journal.pone.0022779.
47. Nomaguchi M, Doi N, Fujiwara S, Saito A, Akari H, Nakayama EE, Shioda T, Yokoyama M, Sato H, Adachi A. 2013. Systemic biological analysis of the mutations in two distinct HIV-1mt genomes occurred during replication in macaque cells. Microbes Infect. 15:319–328.
48. Hatziioannou T, Cowan S, Von Schwedler UK, Sundquist WI, Bieniasz PD. 2004. Species-specific tropism determinants in the human immunodeficiency virus type 1 capsid. J. Virol. 78:6005–6012.
49. Owens CM, Song B, Perron MJ, Yang PC, Stremlau M, Sodroski J. 2004. Binding and susceptibility to postentry restriction factors in monkey cells are specified by distinct regions of the human immunodeficiency virus type 1 capsid. J. Virol. 78:5423–5437.
50. von Schwedler UK, Stray KM, Garrus JE, Sundquist WI. 2003. Functional surfaces of the human immunodeficiency virus type 1 capsid protein. J. Virol. 77:5439–5450.
51. Lim SY, Rogers T, Chan T, Whitney JB, Kim J, Sodroski J, Letvin NL. 2010. TRIM5alpha modulates immunodeficiency virus control in rhesus monkeys. PLoS Pathog. 6:e1000738. doi:10.1371/journal.ppat.1000738.
52. Jia B, Serra-Moreno R, Neidermyer W, Rahmberg A, Mackey J, Fofana IB, Johnson WE, Westmoreland S, Evans DT. 2009. Species-specific activity of SIV Nef and HIV-1 Vpu in overcoming restriction by tetherin/BST2. PLoS Pathog. 5:e1000429. doi:10.1371/journal.ppat.1000429.
53. Zhang F, Wilson SJ, Landford WC, Virgen B, Gregory D, Johnson MC, Munch J, Kirchhoff F, Bieniasz PD, Hatziioannou T. 2009. Nef proteins from simian immunodeficiency viruses are tetherin antagonists. Cell Host Microbe 6:54–67.
54. Vigan R, Neil SJ. 2010. Determinants of tetherin antagonism in the transmembrane domain of the human immunodeficiency virus type 1 Vpu protein. J. Virol. 84:12958–12970.
55. McCarthy KR, Schmidt AG, Kirmaier A, Wyand AL, Newman RM, Johnson WE. 2013. Gain-of-sensitivity mutations in a Trim5-resistant primary isolate of pathogenic SIV identify two independent conserved determinants of Trim5α specificity. PLoS Pathog. 9:e1003352. doi:10.1371/journal.ppat.1003352.
56. Kuroishi A, Saito A, Shingai Y, Shioda T, Nomaguchi M, Adachi A, Akari H, Nakayama EE. 2009. Modification of a loop sequence between alpha-helices 6 and 7 of virus capsid (CA) protein in a human immunodeficiency virus type 1 (HIV-1) derivative that has simian immunodeficiency virus (SIVmac239) vif and CA alpha-helices 4 and 5 loop improves replication in cynomolgus monkey cells. Retrovirology 6:70. doi:10.1186/1742-4690-6-70.
57. Ohkura S, Goldstone DC, Yap MW, Holden-Dye K, Taylor IA, Stoye JP. 2011. Novel escape mutants suggest an extensive TRIM5α binding site spanning the entire outer surface of the murine leukemia virus capsid protein. PLoS Pathog. 7:e1002011. doi:10.1371/journal.ppat.1002011.
58. Homann S, Smith D, Little S, Richman D, Guatelli J. 2011. Upregulation of BST-2/tetherin by HIV infection *in vivo*. J. Virol. 85:10659–10668.
59. Liberatore RA, Bieniasz PD. 2011. Tetherin is a key effector of the antiretroviral activity of type I interferon in vitro and in vivo. Proc. Natl. Acad. Sci. U. S. A. 108:18097–18101.
60. Pillai SK, Abdel-Mohsen M, Guatelli J, Skasko M, Monto A, Fujimoto K, Yukl S, Greene WC, Kovari H, Rauch A, Fellay J, Battegay M, Hirschel B, Witteck A, Bernasconi E, Ledergerber B, Günthard HF, Wong JK, Swiss HIV Cohort Study. 2012. Role of retroviral restriction factors in the interferon-α-mediated suppression of HIV-1 in vivo. Proc. Natl. Acad. Sci. U. S. A. 109:3035–3040.
61. Serra-Moreno R, Jia B, Breed M, Alvarez X, Evans DT. 2011. Compensatory changes in the cytoplasmic tail of gp41 confer resistance to tetherin/BST-2 in a pathogenic nef-deleted SIV. Cell Host Microbe 9:46–57.
62. Goldstein S, Brown CR, Dehghani H, Lifson JD, Hirsch VM. 2000. Intrinsic susceptibility of rhesus macaque peripheral CD4(+) T cells to simian immunodeficiency virus in vitro is predictive of in vivo viral replication. J. Virol. 74:9388–9395.
63. Lifson JD, Nowak MA, Goldstein S, Rossio JL, Kinter A, Vasquez G, Wiltrout TA, Brown C, Schneider D, Wahl L, Lloyd AL, Williams J, Elkins WR, Fauci AS, Hirsch VM. 1997. The extent of early viral replication is a critical determinant of the natural history of simian immunodeficiency virus infection. J. Virol. 71:9508–9514.
64. Igarashi T, Iyengar R, Byrum RA, Buckler-White A, Dewar RL, Buckler CE, Lane HC, Kamada K, Adachi A, Martin MA. 2007. Human immunodeficiency virus type 1 derivative with 7% simian immunodeficiency virus genetic content is able to establish infections in pig-tailed macaques. J. Virol. 81:11549–11552.
65. Lifson JD, Haigwood NL. 2012. Lessons in nonhuman primate models for AIDS vaccine research: from minefields to milestones. Cold Spring Harb. Perspect. Med. 2:a007310. doi:10.1101/cshperspect.a007310.
66. Shaw GM, Hunter E. 2012. HIV transmission. Cold Spring Harb. Perspect. Med. 2:a006965. doi:10.1101/cshperspect.a006965.

67. **Swanstrom R, Coffin J.** 2012. HIV-1 pathogenesis: the virus. Cold Spring Harb. Perspect. Med. **2**:a007443. doi:10.1101/cshperspect.a007443.
68. **Nishimura Y, Shingai M, Willey R, Sadjadpour R, Lee WR, Brown CR, Brenchley JM, Buckler-White A, Petros R, Eckhaus M, Hoffman V, Igarashi T, Martin MA.** 2010. Generation of the pathogenic R5-tropic simian/human immunodeficiency virus $SHIV_{AD8}$ by serial passaging in rhesus macaques. J. Virol. **84**:4769–4781.
69. **Ren W, Mumbauer A, Gettie A, Seaman MS, Russell-Lodrigue K, Blanchard J, Westmoreland S, Cheng-Mayer C.** 2013. Generation of lineage-related, mucosally transmissible subtype C R5 simian-human immunodeficiency viruses capable of AIDS development, induction of neurological disease, and coreceptor switching in rhesus macaques. J. Virol. **87**:6137–6149.
70. **Shingai M, Donau OK, Schmidt SD, Gautam R, Plishka RJ, Buckler-White A, Sadjadpour R, Lee WR, LaBranche CC, Montefiori DC, Mascola JR, Nishimura Y, Martin MA.** 2012. Most rhesus macaques infected with the CCR5-tropic $SHIV_{AD8}$ generate cross-reactive antibodies that neutralize multiple HIV-1 strains. Proc. Natl. Acad. Sci. U. S. A. **109**:19769–19774.
71. **Shibata R, Kawamura M, Sakai H, Hayami M, Ishimoto A, Adachi A.** 1991. Generation of a chimeric human and simian immunodeficiency virus infectious to monkey peripheral blood mononuclear cells. J. Virol. **65**:3514–3520.
72. **Kawamura M, Sakai H, Adachi A.** 1994. Human immunodeficiency virus Vpx is required for the early phase of replication in peripheral blood mononuclear cells. Microbiol. Immunol. **38**:871–878.
73. **Gamble TR, Vajdos FF, Yoo S, Worthylake DK, Houseweart M, Sundquist WI, Hill CP.** 1996. Crystal structure of human cyclophilin A bound to the amino-terminal domain of HIV-1 capsid. Cell **87**:1285–1294.

Structure and Dynamics of the gp120 V3 Loop That Confers Noncompetitive Resistance in R5 HIV-1_{JR-FL} to Maraviroc

Yuzhe Yuan[1], Masaru Yokoyama[2], Yosuke Maeda[3], Hiromi Terasawa[3], Shinji Harada[3], Hironori Sato[2], Keisuke Yusa[4]*

1 Transfusion Transmitted Diseases Center, Institute of Blood Transfusion, Chinese Academy of Medical Science, Chenghua District, Chengdu, Sichuan Province, P. R. China, **2** Pathogen Genomics Center, National Institute of Infectious Diseases, Musashi Murayama, Tokyo, Japan, **3** Department of Medical Virology, Graduate School of Medical Sciences, Kumamoto University, Kumamoto, Japan, **4** Division of Biological Chemistry and Biologicals, National Institute of Health Sciences, Setagaya, Tokyo, Japan

Abstract

Maraviroc, an (HIV-1) entry inhibitor, binds to CCR5 and efficiently prevents R5 human immunodeficiency virus type 1 (HIV-1) from using CCR5 as a coreceptor for entry into $CD4^+$ cells. However, HIV-1 can elude maraviroc by using the drug-bound form of CCR5 as a coreceptor. This property is known as noncompetitive resistance. HIV-$1_{V3\text{-}M5}$ derived from HIV-$1_{JR\text{-}FLan}$ is a noncompetitive-resistant virus that contains five mutations (I304V/F312W/T314A/E317D/I318V) in the gp120 V3 loop alone. To obtain genetic and structural insights into maraviroc resistance in HIV-1, we performed here mutagenesis and computer-assisted structural study. A series of site-directed mutagenesis experiments demonstrated that combinations of V3 mutations are required for HIV-$1_{JR\text{-}FLan}$ to replicate in the presence of 1 μM maraviroc, and that a T199K mutation in the C2 region increases viral fitness in combination with V3 mutations. Molecular dynamic (MD) simulations of the gp120 outer domain V3 loop with or without the five mutations showed that the V3 mutations induced (i) changes in V3 configuration on the gp120 outer domain, (ii) reduction of an anti-parallel β-sheet in the V3 stem region, (iii) reduction in fluctuations of the V3 tip and stem regions, and (iv) a shift of the fluctuation site at the V3 base region. These results suggest that the HIV-1 gp120 V3 mutations that confer maraviroc resistance alter structure and dynamics of the V3 loop on the gp120 outer domain, and enable interactions between gp120 and the drug-bound form of CCR5.

Citation: Yuan Y, Yokoyama M, Maeda Y, Terasawa H, Harada S, et al. (2013) Structure and Dynamics of the gp120 V3 Loop That Confers Noncompetitive Resistance in R5 HIV-$1_{JR\text{-}FL}$ to Maraviroc. PLoS ONE 8(6): e65115. doi:10.1371/journal.pone.0065115

Editor: Jean-Pierre Vartanian, Institut Pasteur, France

Received February 14, 2013; **Accepted** April 21, 2013; **Published** June 28, 2013

Funding: This work was supported by grants from the Ministry of Health, Labour and Welfare and by the Global COE program Education and Research Center Aiming at the Control of AIDS from the Ministry of Education, Science, Sports and Culture, Japan. Y.Y. was supported by National Natural Science Foundation of China (81201329), scholarship for youth from Chinese Academy of Medical Sciences and Peking Union Medical College. The funders had no role in study design, data collection and analysis, decision to publish, or preparation of the manuscript.

Competing Interests: The authors have declared that no competing interests exist.

* E-mail: yusak@nihs.go.jp

Introduction

Inhibiting the entry of R5 human immunodeficiency virus type 1 (HIV-1) into $CCR5^+/CD4^+$ cells is an effective step in blocking viral replication. An entry inhibitor can bind to CCR5 and prevent R5 HIV-1 from using CCR5 as a coreceptor for entry [1]. Maraviroc, a CCR5 antagonist, has potent *in vitro* and *in vivo* antiviral activity against laboratory strains and clinical isolates [2–4]. Maraviroc, approved in 2007, was the first CCR5 antagonist approved by the US Food and Drug Administration and is currently used to treat patients with R5-tropic HIV-1 infections.

Treatment failures can occur because of an increasing number of pre-existing CXCR4-using viruses [5,6]. Alternatively, escape mutants can evade a CCR5 inhibitor by accumulating multiple mutations in gp120 and/or gp41 without switching their coreceptor usage [7–14]. Escape mutants can use the drug-bound form of CCR5 as a coreceptor, a property known as noncompetitive resistance [8,9,11]. In noncompetitive-resistant viruses, drug-free CCR5 usage is compatible with the additional ability of drug-bound CCR5 usage. We previously reported that a combination of polymorphic mutations in the gp120 V3 loop can confer noncompetitive resistance in HIV-$1_{JR\text{-}FL}$ [15]. One of these viruses, designated HIV-$1_{V3\text{-}M5}$, contains a set of five mutations I304V/F312W/T314A/E317D/I318V in the V3 loop (from Cys^{293} to Cys^{327}). Most other noncompetitive-resistant viruses contain multiple mutations in the V3 loop [8,9,11], although mutations reported till date in the V3 loop are not always common and resistance-associated mutations in the V3 loop were considered to be background dependent. Two elements are involved in gp120 coreceptor binding: (i) the V3 tip for the CCR5 extracellular loop 2 (ECL2) and (ii) the V3 base and stem residues and the V3 base of the gp120 core for the CCR5 N terminus [16–19]. Thus, the V3 loop of HIV-1 plays a pivotal role in its interaction with CCR5. However, how the V3 mutations induce maraviroc-resistance without changing coreceptor tropism remains unknown.

Increasing evidence indicates that the protein surface fluctuates in solution, and that such fluctuations play key roles in interactions with other molecules [20][20,23]. We previously suggested that the structural dynamics of the HIV-1 gp120 V3 loop play key roles

in modulating viral interactions with various molecules, including HIV-1 coreceptors and anti-V3 antibodies [21,22]. Therefore, it is conceivable that the V3 mutations that cause changes in the structural dynamics of the V3 loop may also be important for viral interactions with the maraviroc and CCR5 complex.

In this study, we examined how the V3 mutations, which conferred maraviroc resistance in HIV-$1_{JR\text{-}FL}$, affect the structural dynamics of the V3 loop on the gp120 outer domain. We initially performed extensive mutagenesis on the V3 loop to clarify a genetic basis for maraviroc-resistance of the HIV-$1_{JR\text{-}FL}$ strain. These studies demonstrated that combinations of V3 mutations are required to render maraviroc resistance to HIV-$1_{JR\text{-}FL}$. Subsequently, we performed MD simulations [23–25] of HIV-$1_{JR\text{-}FL}$ gp120 outer domains carrying V3 loops with and without the five maraviroc resistance mutations. The results illustrate that at the atomic-level maraviroc resistance mutations affect intrinsic structural properties and motion of the V3 loop on the HIV-1 gp120 outer domain.

Materials and Methods

Cells and Viruses

PM1/CCR5 cells were generated from the human $CD4^+$ T-cell line PM1 [26] by standard retrovirus-mediated transduction with pG1TKneo-CCR5 [27]. The cells were maintained in RPMI 1640 (Invitrogen) supplemented with 10% heat-inactivated fetal calf serum (FCS; Vitromex). MAGIC-5 cells (HeLa-$CD4^+$-$CCR5^+$-LTR-b-galactosidase) [28], used as reporter cells for HIV-1 infection, and 293T cells were maintained in Dulbecco's modified Eagle's medium (ICN Biomedicals) supplemented with 10% heat-inactivated FCS. pJR-FL was kindly provided by Prof. Koyanagi (Kyoto University).

MD simulation

HIV-1 gp120 outer domain structures with various V3 regions were constructed by the homology modeling method, using Molecular Operating Environment (MOE) software v. 2010.10 (Chemical Computing Group Inc., Montreal, Quebec, Canada) [22]. For the modeling template, we used the crystal structure of HIV-1 gp120 containing an entire V3 region at a resolution of 3.30 Å (PDB code: 2QAD) [29]. The 186 amino-terminal and 27 carboxyl-terminal residues were deleted to construct the gp120 outer domain structure. MD simulations were performed using the SANDER module of the AMBER 9 program package [30], the AMBER99SB force field [31], and the TIP3P water model [32]. Bond lengths involving hydrogen were constrained using SHAKE algorithm [32] and the time for all MD simulations was set to 2 fs. A nonbonded cutoff of 12 Å was used. After heating calculations for 20 ps until 310 K using the NVT ensemble, simulations were conducted with the NPT ensemble at 1 atm and 310 K for 20 ns. Superimposition of structures was performed by coordinating the atoms of the amino acids along the β-sheet at the gp120 core. We calculated the root mean square fluctuation (RMSF) to determine the atomic fluctuations along the trajectory broken down by residues during MD simulations. Average structures during the final 10 ns of MD simulations were used as reference structures. RMSFs were calculated using the ptraj module of AMBER 9 [22].

V3 mutant viruses

V3 mutant proviruses were constructed from pJR-FL_{an}. The 176-bp DNA fragments containing single mutations (I304V, F312W, T314A, E317D, or I318V) were subcloned into a cloning vector by overlapping PCR using primers tagged with a mutated tail. The mutation-containing DNA fragments encoding the V3 loop were repeatedly amplified from the cloning vectors using the primers VV-Af (5′-ACAGCTTAAGGAATC TGTAGAAAT-TAATTG-3′) and VV-Nh (5′-ATTTGCTAGCTATC TGTTTTAAAGTGTCAT-3′). Products were digested with AflII and NheI, subcloned into pCR-SXΔAN, and designated as pCR-SX_1, pCR-SX_2, pCR-SX_3, pCR-SX_4, and pCR-SX_5. The *Stu* I–*Xho* I fragment from the plasmids was then subcloned into pJR-FLΔSX that was created by replacing the *Stu* I–*Xho* I fragment of pJR-FL with a linker. The end products were proviral plasmids that were used for transfection for virus production. The procedure described above was repeated for construction of the proviral DNA containing two to four mutations.

For virus preparation, 293T cells (2×10^6) were transfected with 10 μg of proviral DNA using the calcium phosphate ProFection Mammalian Transfection System (Promega). The supernatant was collected 28 h after transfection, filtered through a 0.22-μm filter (Millipore), and stored at −80°C until further use. The amount of p24 Gag in the supernatant was measured by p24 Gag ELISA (Zeptometrix).

Viral replication assay

For the viral replication assay, 4×10^4 PM1/CCR5 cells were infected with 8 ng p24 Gag for 2 h in the presence or absence of 1 μM maraviroc. After washing twice with phosphate-buffered saline (PBS), the infected cells were incubated at 37°C in a 5% CO_2 atmosphere in the presence or absence of 1 μM maraviroc. On day 6 after infection, the amount of p24 Gag in the supernatant was measured by p24 Gag ELISA (Zeptometrix). Maraviroc was provided by the NIH AIDS Research and Reference Reagent Program, Division of AIDS National Institute of Allergy and Infectious Diseases.

Determination of drug susceptibility

Drug susceptibilities were determined by the single-round viral entry assay using previously titrated pseudotyped virus preparations with MAGIC-5 cells. In brief, MAGIC-5 cells were plated in 48-well tissue culture plates 1 day before infection. After absorption of the pseudotyped virus for 2 h at 37°C in the presence or absence of 1 μM maraviroc, the cells were washed twice with PBS and further incubated for 48 h in fresh medium in the presence or absence of the inhibitor.

HIV-1 single-cycle luciferase reporter assay

HIV-1 single-cycle luciferase reporter viruses were produced by cotransfection of 293T cells with pNL–LucR–E^- [33] and Env-expressing plasmids pCXN–EnvJR-FLan, pCXN–$Env_{V3\text{-}M5}$, pCXN–Env_{2345}, pCXN–Env_{1345}, pCXN–Env_{1245}, pCXN–Env_{1235}, or pCXN–Env_{1234}. Culture supernatant containing pseudoviruses at a final concentration of 1 ng/ml p24 was added to 1×10^4 cells/well MAGIC5 cells [28] in a 48-well plate. After 2 h, the cells were washed twice with phosphate-buffered saline (PBS) and firefly luciferase activity was measured 48 h postinfection, according to the manufacturer's directions (Promega).

Results

Noncompetitive-resistant virus HIV-$1_{V3\text{-}M5}$

HIV-$1_{V3\text{-}M5}$ containing the five mutations I304V/F312W/T314A/E317D/I318V in the V3 loop with a JR-FL background (Figure 1A) exhibits noncompetitive resistance to maraviroc [15]. This virus could replicate in the presence of an extremely high concentration of the entry inhibitor (Figure 1B), i.e., 1 μM maraviroc, which was 147-fold higher than the IC_{50} value of the wild-type HIV-$1_{JR\text{-}FLan}$ (0.0069 μM). HIV-$1_{V3\text{-}M5}$ could infect

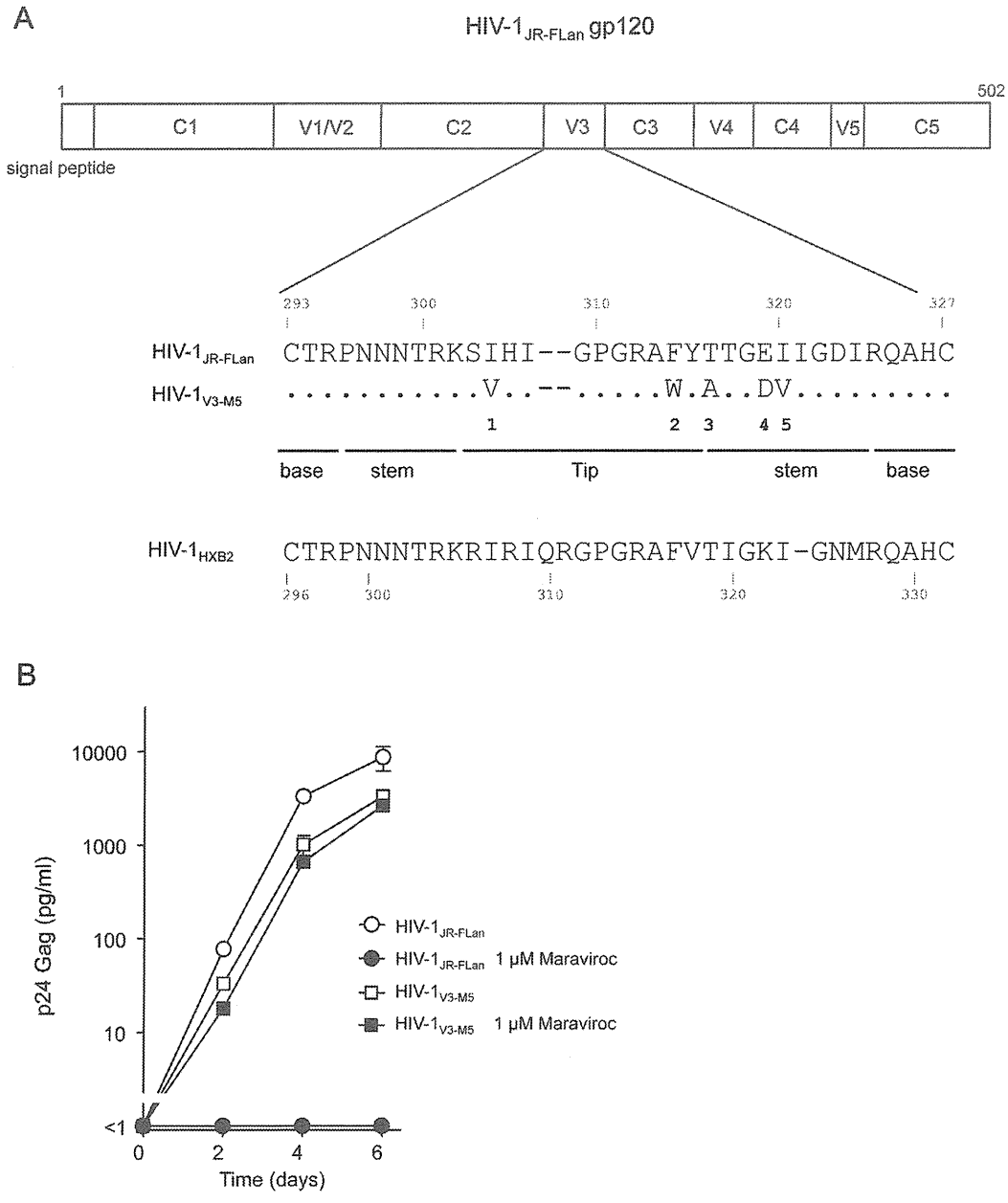

Figure 1. Noncompetitive resistant HIV-$1_{V3\text{-}M5}$. (A) Five amino acid substitutions in the V3 loop of HIV-$1_{V3\text{-}M5}$ (I304V/F312W/T314A/E317D/I318V). HIV-$1_{JR\text{-}FLan}$ was created form HIV-$1_{JR\text{-}FL}$ by incorporation of AflII and NheI. Incorporation of the NheI site led to amino acid substitutions Val^{342}-Ile^{343} to Ala^{342}-Ser^{343}. HIV-$1_{JR\text{-}FLan}$ was used as the parental virus. (B) Replication kinetics of HIV-$1_{V3\text{-}M5}$ in the presence or absence of 1 μM maraviroc in PM1/CCR5 cells. PM1/CCR5 cells (1×10^5) were infected with 10 ng of p24 Gag for 3 h. Viral replication was monitored by measuring p24 Gag in the supernatant after infection. The analysis was repeated three times; the error bars represent the S.D. of three replicates from one representative experiment.
doi:10.1371/journal.pone.0065115.g001

PM1/CCR5 cells through drug-bound CCR5 to produce p24 Gag in the presence or absence of 1 μM maraviroc, whereas HIV-$1_{JR\text{-}FLan}$ replication was completely suppressed.

Suppression of replication in recombinant viruses containing one to three mutations in the V3 loop by maraviroc

To further examine the contribution of each mutation to noncompetitive resistance, we constructed recombinant viruses containing one of the five mutations in the V3 loop (Figure 2A). I304V, F312W, T314A, E317D, and I318V were the polymorphic mutations detected in R5 clinical isolates. Thus, none of these viruses exhibited defective growth, although F312W caused a moderate decrease in p24 Gag production in the absence of maraviroc. HIV-$1_{V3\text{-}M5}$ replication was 1.8-fold lower than HIV-$1_{JR\text{-}FLan}$ replication. The presence of 1 μM maraviroc completely suppressed the production of recombinant viruses containing a single mutation, indicating that these single mutations could not confer noncompetitive resistance. Following this, we constructed 11 recombinant viruses, each containing two or three random combinations of the mutations (Figure 2B). Theoretically, the total

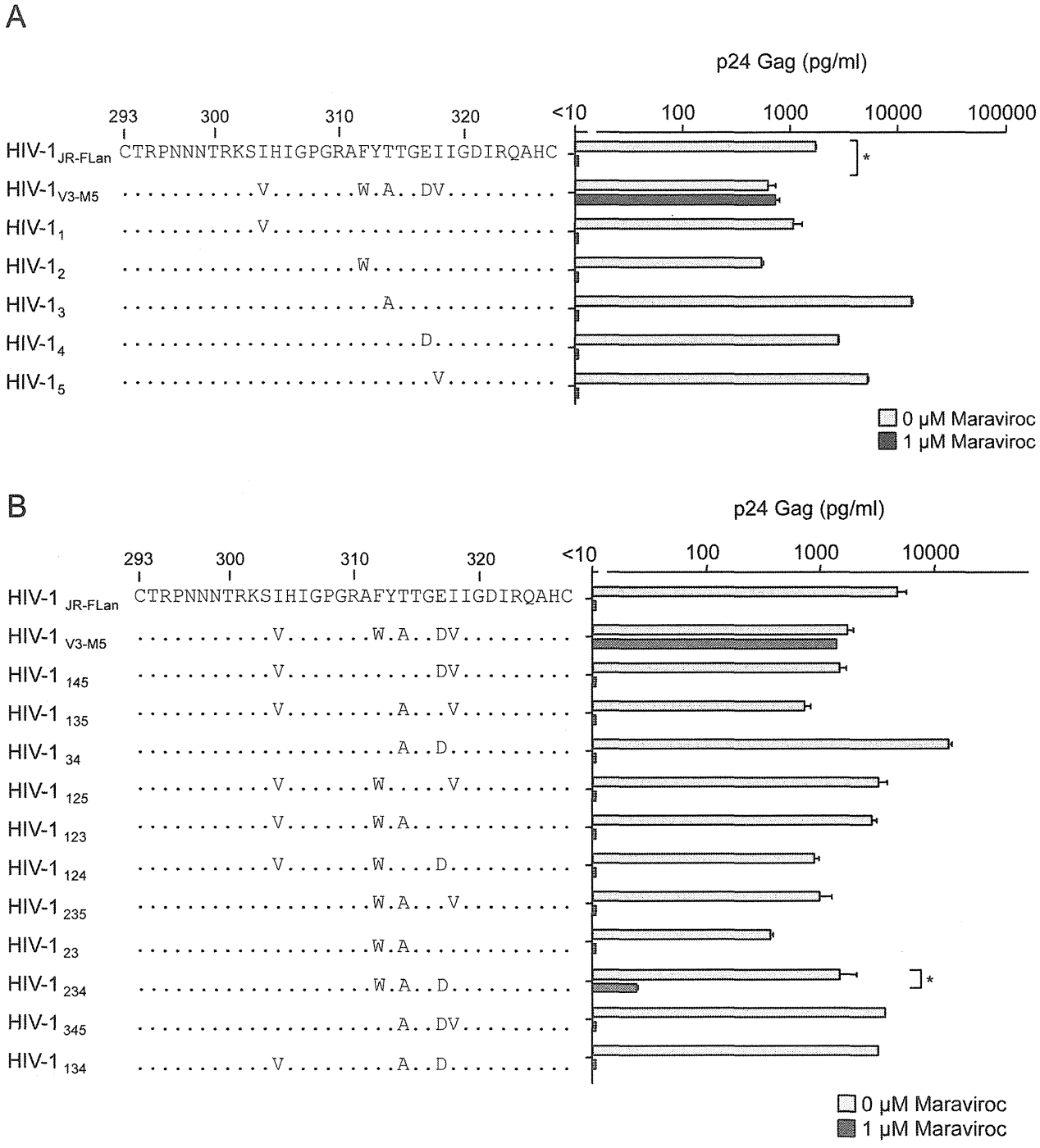

Figure 2. The effect of 1 μM of maraviroc on p24 Gag production in recombinant viruses containing one (A) and two or three (B) of the five amino acid substitutions. PM1/CCR5 cells (1×10^5) were infected with 10 ng p24 Gag for 3 h in the presence or absence of 1 μM maraviroc. On day 6 after infection, the amount of Gag in the supernatant was measured using HIV-1 p24 ELISA. The analysis was repeated three times; the error bars represent the S.D. of three replicates from one representative experiment. **, $p<0.01$. Statistical significant difference was calculated by *t* test.
doi:10.1371/journal.pone.0065115.g002

number of possible combinations of the five mutations was 120; therefore, 11 combinations of two or three mutations were insufficient to determine the crucial combination(s) for noncompetitive resistance. These recombinants could produce more than 100 pg/ml p24 Gag in the absence of maraviroc, although their replication resulted in variable levels of p24 Gag. Maraviroc mostly suppressed the replication of these recombinant viruses, indicating that the combination of these two or three mutations did not confer use of drug-bound CCR5 as a coreceptor for viral entry. However HIV-1_{234} containing F312W/T314A/E317D could replicate in the presence of 1 μM maraviroc, although p24 Gag production was 1.8% of that in its absence. We could not

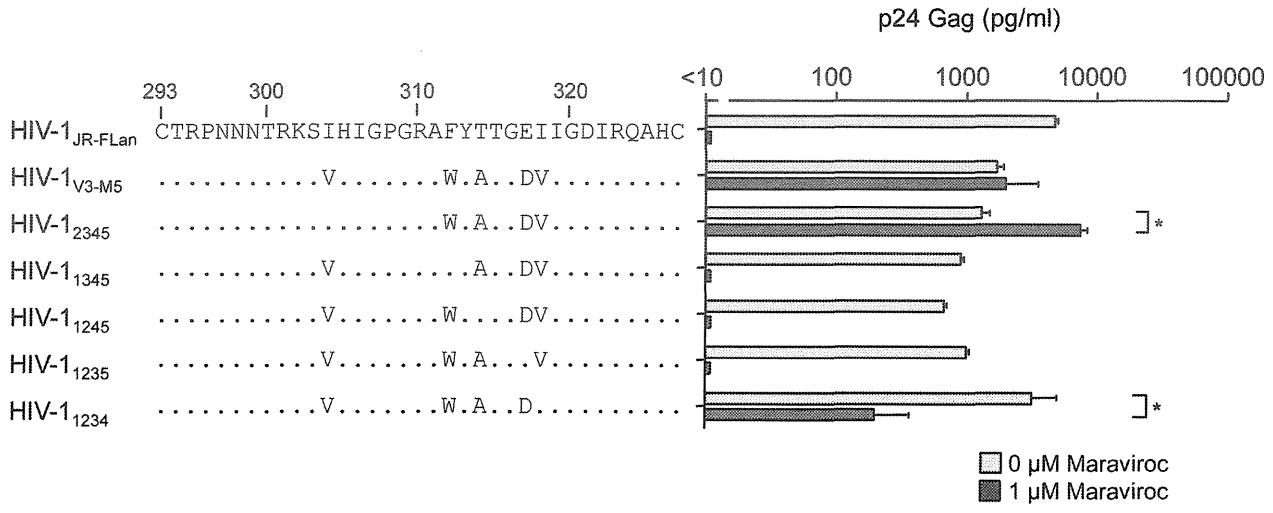

Figure 3. The effect of 1 μM of maraviroc on p24 Gag production in recombinant viruses containing four of the five amino acid substitutions. PM1/CCR5 cells (1×10^5) were infected with 10 ng p24 Gag for 3 h in the presence or absence of 1 μM maraviroc. On day 6 after infection, the amount of Gag in the supernatant was measured using HIV-1 p24 ELISA. The analysis was repeated three times; the error bars represent the S.D. of three replicates from one representative experiment. **, $p<0.01$. Statistical significant difference was calculated by *t* test.
doi:10.1371/journal.pone.0065115.g003

passage HIV-1_{234} in PM1/CCR5 cells because of its poor replication in the presence of 1 μM maraviroc (data not shown). These results suggest that HIV-1_{234} is an intermediate form in the transition of the wild type to a completely noncompetitive-resistant form.

Effect of maraviroc on recombinant viruses containing four mutations in the V3 loop

We next examined the recombinant viruses containing four mutations in the V3 loop (Figure 3). Without maraviroc, the viral fitness of HIV-1_{1234} was comparable with that of HIV-$1_{JR\text{-}FLan}$, whereas the other four recombinant viruses replicated at levels lower than those of HIV-$1_{V3\text{-}M5}$. Of note, HIV-1_{2345} and HIV-1_{1234} could replicate in the presence of 1 μM maraviroc, although HIV-1_{1345}, HIV-1_{1245}, and HIV-1_{1235} replication was completely suppressed. p24 Gag production by HIV-1_{2345} in the presence of maraviroc was 4.5-fold higher than that in its absence, whereas HIV-1_{1234} replication in the presence of maraviroc was 15-fold lower than that in the absence of maraviroc. These two viruses contained three common mutations: F312W, T314A, and E317D.

Effect of maraviroc on recombinant virus containing F312W/T314A/E317D in the V3 loop

We further examined whether HIV-1_{234} containing the triplet mutation F312W/T314A/E317D exhibited noncompetitive resistance (Figure 4). HIV-$1_{V3\text{-}M5}$ replication can be enhanced by T199K in V3 mutants to a level comparable with that in HIV-$1_{JR\text{-}FL}$ [15]. p24 Gag production by HIV-$1_{V3\text{-}M5/T199K}$ increased from 3100 pg/ml to 10,500 pg/ml in the presence of 1 μM maraviroc, whereas there was no significant increase in its absence. Similarly, HIV-$1_{234/T199K}$ replication was significantly enhanced from 31 pg/ml to 650 pg/ml in the presence of 1 μM maraviroc but not in its absence. These results indicated that triplet mutations in the V3 loop are crucial for noncompetitive resistance, and I304V, I318V, or T199K can increase viral fitness.

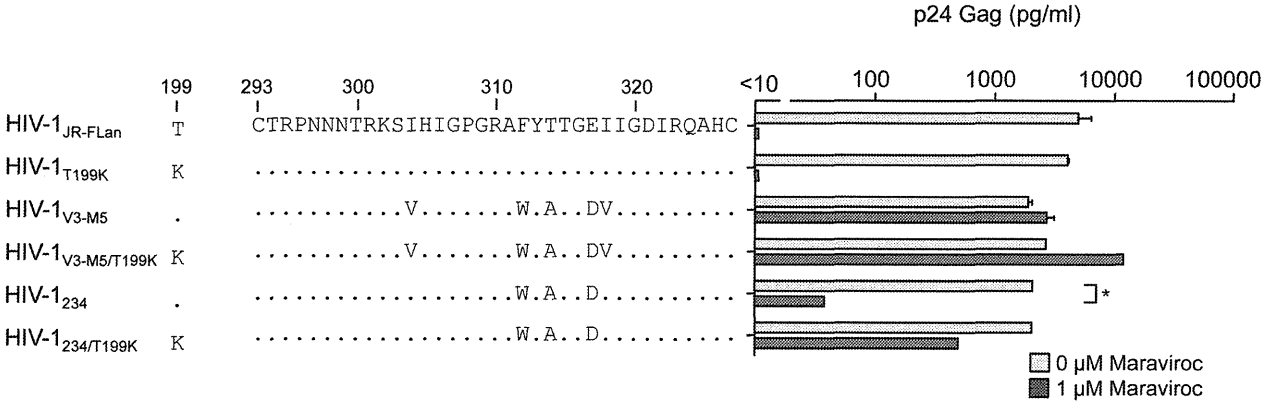

Figure 4. The effect of 1 μM of maraviroc on p24 Gag production in HIV-$1_{JR\text{-}FLan}$, HIV-1_{T199K}, HIV-$1_{V3\text{-}M5}$, HIV-$1_{V3\text{-}M5/T199K}$, HIV-1_{234}, and HIV-$1_{234/T199K}$. PM1/CCR5 cells (1×10^5) were infected with 10 ng p24 Gag for 3 h in the presence or absence of 1 μM maraviroc. On day 6 after infection, the amount of Gag in the supernatant was measured using HIV-1 p24 ELISA. The analysis was repeated three times; the error bars represent the S.D. of three replicates from one representative experiment. **, $p<0.01$. Statistical significant difference was calculated by *t* test.
doi:10.1371/journal.pone.0065115.g004

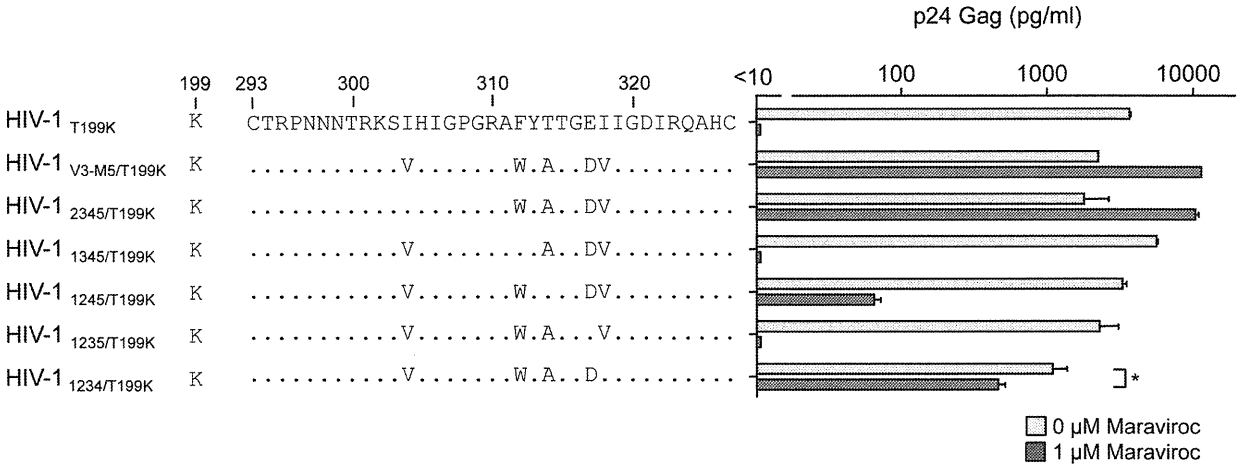

Figure 5. The effect of 1 μM of maraviroc on p24 Gag production in recombinant viruses containing four amino acid substitutions plus T199K. PM1/CCR5 cells (1×10^5) were infected with 10 ng p24 Gag for 3 h in the presence or absence of 1 μM maraviroc. On day 6 after infection, the amount of Gag in the supernatant was measured by HIV-1 p24 ELISA. The analysis was repeated three times; the error bars represent the S.D. of three replicates from one representative experiment. *, $p<0.05$; **, $p<0.01$. Statistical significant difference was calculated by *t* test.
doi:10.1371/journal.pone.0065115.g005

Finally, we examined the effects of T199K on the replication of recombinant viruses carrying four mutations in the V3 loop. In the presence of maraviroc, HIV-1_{1234} produced 6.7% of p24 Gag of that in its absence (Figure 3); however, HIV-$1_{1234/T199K}$ replication increased up to 43% (Figure 5). Of note, HIV-1_{1245} replication was completely suppressed by 1 μM maraviroc (Figure 3); however, HIV-$1_{1245/T199K}$ could replicate in the presence of 1 μM maraviroc, although the p24 production was only 2% of that in the absence maraviroc (Figure 5). These results indicated that the absence of T314A in the triplet could be compensated by I304V, I318V, or T199K and result in noncompetitive resistance.

Susceptibilities of pseudotyped viruses containing four mutations in the V3 loop to maraviroc

To confirm the phenotypes of the recombinant viruses determined by the single-round infection assay using MAGIC-5 cells, we examined the susceptibility of viral entry using pseudotyped viruses with mutant envelopes (Figure 6). The viral entry of HIV-$1_{JR\text{-}FLan}$ Env, HIV-1_{1345} Env, or HIV-1_{1235} Env was completely suppressed by maraviroc. These results were consistent with those obtained using competent viruses (Figure 3). HIV-$1_{V3\text{-}M5}$ Env inhibition with maraviroc saturated approximately 17% entry efficiency [15]. HIV-1_{1234} Env retained 4% entry efficiency in the presence of 1 μM maraviroc, indicating that the low efficiency of drug-bound CCR5 usage accounted for the low replication rate of the competent virus. In contrast, HIV-1_{2345} Env could infect MAGIC-5 cells with 41% entry efficiency of that in the absence of maraviroc (Figure 6), although viral fitness in the presence of the inhibitor was superior to that in its absence in PM1/CCR5 cells (Figure 3). Furthermore, even 1 μM maraviroc did not completely suppress HIV-1_{1245} Env entry (Figure 6). These discrepancies may have occurred because of the cell-type-specific nature of noncompetitive resistance [34].

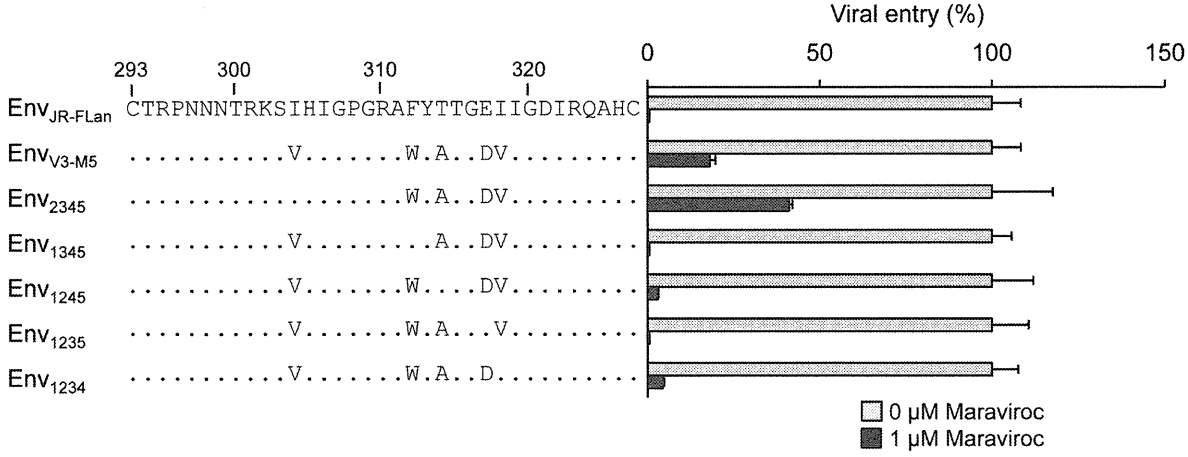

Figure 6. Maraviroc susceptibility of pseudotyped viruses derived from HIV-$1_{JR\text{-}FLan}$, HIV-$1_{V3\text{-}M5}$, HIV-1_{2345}, and HIV-1_{1345}, HIV-1_{1245}, HIV-1_{1235}, and HIV-1_{1234}. MAGIC-5 cells were infected with pseudotyped viruses in the absence or presence of 1 μM maraviroc. The analysis was repeated three times; the error bars represent the S.D. of three replicates from one representative experiment. **, $p<0.01$. Statistical significant difference was calculated by *t* test.
doi:10.1371/journal.pone.0065115.g006

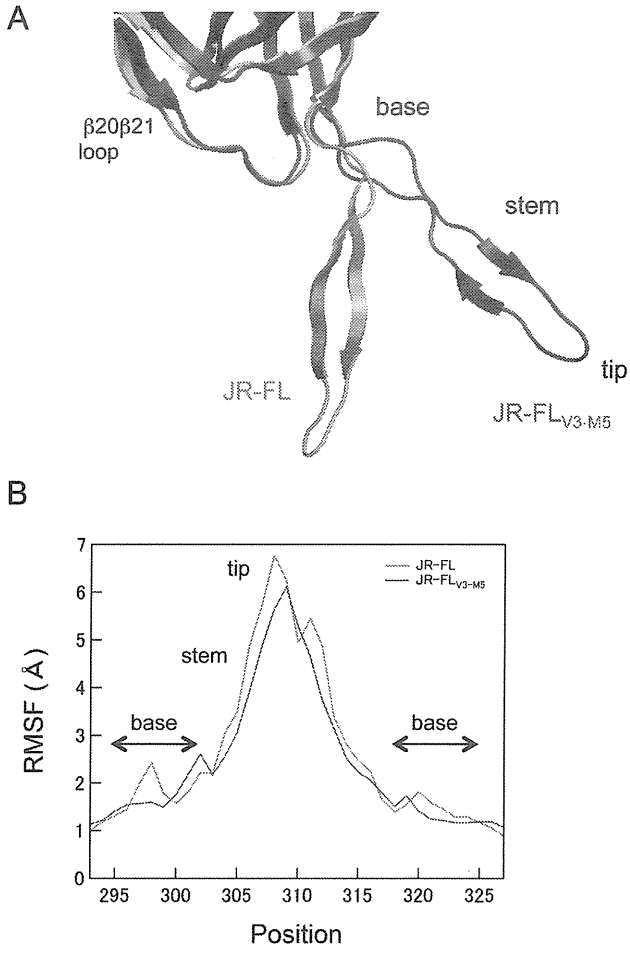

Figure 7. MD simulation of the HIV-1 gp120 outer domain. (A) Superimposition of averaged structures obtained from 40,000 snapshots during the 10–20 ns of MD simulation. Grey and blue ribbons indicate the gp120 V3 of JR-FL$_{an}$ and JR-FL$_{V3-M5}$, respectively. (B) Distribution of RMSF in the V3 region of gp120. The RMSF values indicate the atomic fluctuations of the main chains of individual amino acids during the 10–20 ns of MD simulations.
doi:10.1371/journal.pone.0065115.g007

MD simulations of the HIV-1 gp120 outer domain

MD simulation is a powerful computational method for studying motions of proteins at the atomic-scale [23–25]. To address structural impacts of the V3 maraviroc-resistance mutations, we performed MD simulations of the HIV-1$_{JR-FL}$ gp120 outer domain V3 loop with and without the five mutations of HIV-1$_{V3-M5}$ (I304V/F312W/T314A/E317D/I318V). As described previously [21,22], the root mean square deviation (RMSD) between the initial model and the model at a given time of MD simulation sharply increased soon after heating the initial model and then fluctuated continually for 20 ns of simulations (data not shown). The data suggests an intrinsic property of the gp120 outer domain V3 loops that results in structural fluctuations in solution. Hence, we constructed averaged gp120 structures using 40,000 snapshots during the 10–20 ns of MD simulation, and we superimposed them to reveal structural differences in the V3 loops of the two gp120s. Marked changes in V3 conformation were induced by introduction of the five V3 mutations (Figure 7A). The V3 loop of JR-FL$_{V3-M5}$ was located at a much more distant position from the β20β21 loop in the outer domain than that of JR-FL. In addition, an anti-parallel β-sheet in the V3 stem region was reduced in the V3 loop of JR-FL$_{V3-M5}$ compared with that of JR-FL.

To map the V3 loop sites in which fluctuations are influenced by the five mutations, we calculated the root mean square fluctuation (RMSF) of the main chains of individual amino acids in the V3 loop using 40,000 snapshots from 10–20 ns of each MD simulation (Figure 7B). The RMSF values were maximal at the V3 tip, indicating that the region involved in binding to CCR5 ECL2 fluctuates the most in solution. Interestingly, the five mutations were found to decrease the RMSF throughout the V3 tip and stem regions (Figure 7B, blue line). In addition, the five mutations caused a shift in small RMSF peaks at V3 base regions.

Discussion

In this study, we examined the genetic and structural bases for the noncompetitive resistance of HIV-1 to maraviroc. Using site-directed mutagenesis, we demonstrated that combinations of mutations in V3 are required to confer maraviroc resistance to the HIV-1$_{JR-FL}$ strain (Figures 2, 3). In addition, we showed that in combination with the V3 mutations, a T199K mutation in the C2 region enhanced viral fitness (Figures 4, 5). Finally, we indicated that these five maraviroc-resistance V3 mutations of HIV-1$_{V3-M5}$ change the intrinsic structures and motion of the V3 loop on the HIV-1 gp120 outer domain. These data provide novel insights into the molecular mechanisms of HIV-1 maraviroc resistance. Further study may be able to classify the structure of V3 loop of HIV-1 to reveal or easily develop noncompetitive resistance through antiviral treatment with maraviroc in advance.

In the V3 loop, maraviroc-associated mutations have been reported at His^{305}, Pro^{308}, Ala^{311}, Phe^{312}, Thr^{314}, Glu^{317}, and Ile^{318} (numbering in JR-FL) [11,35–37]. In the HIV-1$_{JR-FLan}$ background, F312W/T314A/E317D is a crucial combination for maraviroc resistance, and I318V was required for extensive replication comparable with that in the wild type (Figure 5). HIV-1$_{234}$ could not be passaged in PM1/CCR5 cells in the presence of 1 μM maraviroc because of its poor viral fitness (data not shown), suggesting that F312W/T314A/E317D is a type of fitness "valley" that needs to be selected on the genetic pathway for the development of noncompetitive resistance. F312W/T314A/E317D and one other mutation are required to acquire noncompetitive resistance. We could not select a maraviroc-resistant virus from the homogeneous viral population of HIV-1$_{JR-FLan}$ because spontaneous multiple mutations ($\geq$4) were unlikely to occur during *in vitro* passages, whereas our V3 virus library inherently contained F312W/T314A/E317D and fitness-enhancing mutations (I304V/I318V) [15]. We could not observe the condensation of viral clones containing one or two of these mutations at low concentrations of maraviroc (0.03–0.1 μM), suggesting that one or two combinations of these mutations did not confer a selective advantage (Figure 2). HIV-1 did not acquire maraviroc resistance by following a pathway for increasing resistance by the accumulation of multiple mutations. Instead, spontaneous alterations in the V3 loop were required to utilize maraviroc-bound CCR5. These results suggest that a virus library containing various mutations in specific regions such as the V3 loop is suitable for the *in vitro* selection of viruses resistant to entry inhibitors [38].

It remains unclear how the maraviroc resistant viruses use maraviroc-bound CCR5 as an entry coreceptor. Accumulating evidence from the investigations of protein chemistry indicates that structural fluctuations of the protein surface in solution play key roles in these molecular interactions [23–25]. Therefore, it is possible that the resistant viruses adjust these structural fluctua-

tions of coreceptor binding surfaces through V3 mutations that enable binding to maraviroc-bound CCR5. In general, it is difficult to analyze motions of proteins at an atomic scale. However, recent advances in hardware and software of biomolecular simulation have rapidly improved its precision and performance [23–25]. Therefore, in this study we applied MD simulations and elucidated the structural dynamics of the gp120 outer domain in solution.

Our MD simulations of the gp120 outer domain suggest that the five mutations in the V3 loop of HIV-$1_{V3\text{-}M5}$ caused marked changes in the physical properties of the CCR5 binding surface (Figure 7). Firstly, the mutations altered configurations and secondary structure of the tip-stem region of V3 loop on gp120. Secondly, the mutations reduced fluctuations at the base and tip regions of the V3 loop on gp120 and shifted the site of these fluctuations to the V3 base region. These results illustrate how maraviroc-resistance mutations have an impact on the intrinsic properties and structural motions of the V3 loops on the HIV-1 gp120 outer domain at the atomic-level. The altered configuration and/or fluctuation of the mutant V3 loops may advantageously support binding to drug-bound CCR5 by attenuating fluctuations on its surface. Further MD simulations in combination with experiments will clarify which of these structural changes are critical for the maraviroc resistance of HIV-1.

Author Contributions

Conceived and designed the experiments: YY KY. Performed the experiments: YY MY YM HT SH. Analyzed the data: YY MY YM SH HS KY. Contributed reagents/materials/analysis tools: YY MY YM SH HS KY. Wrote the paper: YY HS KY.

References

1. Tilton JC, Wilen CB, Didigu CA, Sinha R, Harrison JE, et al. (2010) A maraviroc-resistant HIV-1 with narrow cross-resistance to other CCR5 antagonists depends on both N-terminal and extracellular loop domains of drug-bound CCR5. J Virol 84: 10863–10876.
2. Fadel H, Temesgen Z (2007) Maraviroc. Drugs Today (Barc) 43: 749–758.
3. Tilton JC, Doms RW (2010) Entry inhibitors in the treatment of HIV-1 infection. Antiviral Res 85: 91–100.
4. Gorry PR, Ancuta P (2011) Coreceptors and HIV-1 pathogenesis. Curr HIV/AIDS Rep 8: 45–53.
5. Gulick RM, Su Z, Flexner C, Hughes MD, Skolnik PR, et al. (2007) Phase 2 study of the safety and efficacy of vicriviroc, a CCR5 inhibitor, in HIV-1-Infected, treatment-experienced patients: AIDS clinical trials group 5211. J Infect Dis 196: 304–312.
6. Moore JP, Kuritzkes DR (2009) A piece de resistance: how HIV-1 escapes small molecule CCR5 inhibitors. Curr Opin HIV AIDS 4: 118–124.
7. Westby M, van der Ryst E (2010) CCR5 antagonists: host-targeted antiviral agents for the treatment of HIV infection, 4 years on. Antivir Chem Chemother 20: 179–192.
8. Kuhmann SE, Pugach P, Kunstman KJ, Taylor J, Stanfield RL, et al. (2004) Genetic and phenotypic analyses of human immunodeficiency virus type 1 escape from a small-molecule CCR5 inhibitor. J Virol 78: 2790–2807.
9. Trkola A, Kuhmann SE, Strizki JM, Maxwell E, Ketas T, et al. (2002) HIV-1 escape from a small molecule, CCR5-specific entry inhibitor does not involve CXCR4 use. Proc Natl Acad Sci U S A 99: 395–400.
10. Marozsan AJ, Kuhmann SE, Morgan T, Herrera C, Rivera-Troche E, et al. (2005) Generation and properties of a human immunodeficiency virus type 1 isolate resistant to the small molecule CCR5 inhibitor, SCH-417690 (SCH-D). Virology 338: 182–199.
11. Westby M, Smith-Burchnell C, Mori J, Lewis M, Mosley M, et al. (2007) Reduced maximal inhibition in phenotypic susceptibility assays indicates that viral strains resistant to the CCR5 antagonist maraviroc utilize inhibitor-bound receptor for entry. J Virol 81: 2359–2371.
12. Pugach P, Marozsan AJ, Ketas TJ, Landes EL, Moore JP, et al. (2007) HIV-1 clones resistant to a small molecule CCR5 inhibitor use the inhibitor-bound form of CCR5 for entry. Virology 361: 212–228.
13. Baba M, Miyake H, Wang X, Okamoto M, Takashima K (2007) Isolation and characterization of human immunodeficiency virus type 1 resistant to the small-molecule CCR5 antagonist TAK-652. Antimicrob Agents Chemother 51: 707–715.
14. Ogert RA, Wojcik L, Buontempo C, Ba L, Buontempo P, et al. (2008) Mapping resistance to the CCR5 co-rceceptor antagonist vicriviroc using heterologous chimeric HIV-1 envelope genes reveals key determinants in the C2-V5 domain of gp120. Virology 373: 387–399.
15. Yuan Y, Maeda Y, Terasawa H, Monde K, Harada S, et al. (2011) A combination of polymorphic mutations in V3 loop of HIV-1 gp120 can confer noncompetitive resistance to maraviroc. Virology 413: 293–299.
16. Rizzuto CD, Wyatt R, Hernandez-Ramos N, Sun Y, Kwong PD, et al. (1998) A conserved HIV gp120 glycoprotein structure involved in chemokine receptor binding. Science 280: 1949–1953.
17. Rizzuto C, Sodroski J (2000) Fine definition of a conserved CCR5-binding region on the human immunodeficiency virus type 1 glycoprotein 120. AIDS Res Hum Retroviruses 16: 741–749.
18. Cormier EG, Dragic T (2002) The crown and stem of the V3 loop play distinct roles in human immunodeficiency virus type 1 envelope glycoprotein interactions with the CCR5 coreceptor. J Virol 76: 8953–8957.
19. Cormier EG, Tran DN, Yukhayeva L, Olson WC, Dragic T (2001) Mapping the determinants of the CCR5 amino-terminal sulfopeptide interaction with soluble human immunodeficiency virus type 1 gp120-CD4 complexes. J Virol 75: 5541–5549.
20. Thorpe IF, Brooks CL 3rd (2007) Molecular evolution of affinity and flexibility in the immune system. Proc Natl Acad Sci U S A 104: 8821–8826.
21. Yokoyama M, Naganawa S, Yoshimura K, Matsushita S, Sato H (2012) Structural dynamics of HIV-1 envelope Gp120 outer domain with V3 loop. PLoS One 7: e37530.
22. Naganawa S, Yokoyama M, Shiino T, Suzuki T, Ishigatsubo Y, et al. (2008) Net positive charge of HIV-1 CRF01_AE V3 sequence regulates viral sensitivity to humoral immunity. PLoS One 3: e3206.
23. Ode H, Nakashima M, Kitamura S, Sugiura W, Sato H (2012) Molecular dynamics simulation in virus research. Front Microbiol 3: 258.
24. Karplus M, Kuriyan J (2005) Molecular dynamics and protein function. Proc Natl Acad Sci U S A 102: 6679–6685.
25. Dodson GG, Lane DP, Verma CS (2008) Molecular simulations of protein dynamics: new windows on mechanisms in biology. EMBO Rep 9: 144–150.
26. Lusso P, Earl PL, Sironi F, Santoro F, Ripamonti C, et al. (2005) Cryptic nature of a conserved, CD4-inducible V3 loop neutralization epitope in the native envelope glycoprotein oligomer of CCR5-restricted, but not CXCR4-using, primary human immunodeficiency virus type 1 strains. J Virol 79: 6957–6968.
27. Maeda Y, Foda M, Matsushita S, Harada S (2000) Involvement of both the V2 and V3 regions of the CCR5-tropic human immunodeficiency virus type 1 envelope in reduced sensitivity to macrophage inflammatory protein 1alpha. J Virol 74: 1787–1793.
28. Hachiya A, Aizawa-Matsuoka S, Tanaka M, Takahashi Y, Ida S, et al. (2001) Rapid and simple phenotypic assay for drug susceptibility of human immunodeficiency virus type 1 using CCR5-expressing HeLa/CD4(+) cell clone 1–10 (MAGIC-5). Antimicrob Agents Chemother 45: 495–501.
29. Huang CC, Tang M, Zhang MY, Majeed S, Montabana E, et al. (2005) Structure of a V3-containing HIV-1 gp120 core. Science 310: 1025–1028.
30. Case DA, TAD, Cheatham III TE, Simmerling CL, Wang JM, et al. (2006) AMBER 9. San Francisco: University of California.
31. Hornak V, Abel R, Okur A, Strockbine B, Roitberg A, et al. (2006) Comparison of multiple Amber force fields and development of improved protein backbone parameters. Proteins 65: 712–725.
32. Jorgensen WL, Chandrasekhar J, Madura JD, Impey RW, Klein ML (1983) Comparison of simple potential functions for simulating liquid water. J Chem Phys 79: 926–935.
33. Mariani R, Rutter G, Harris ME, Hope TJ, Krausslich HG, et al. (2000) A block to human immunodeficiency virus type 1 assembly in murine cells. J Virol 74: 3859–3870.
34. Roche M, Jakobsen MR, Sterjovski J, Ellett A, Posta F, et al. (2011) HIV-1 escape from the CCR5 antagonist maraviroc associated with an altered and less-efficient mechanism of gp120-CCR5 engagement that attenuates macrophage tropism. J Virol 85: 4330–4342.
35. Tilton JC, Amrine-Madsen H, Miamidian JL, Kitrinos KM, Pfaff J, et al. (2010) HIV type 1 from a patient with baseline resistance to CCR5 antagonists uses drug-bound receptor for entry. AIDS Res Hum Retroviruses 26: 13–24.
36. Maeda Y, Yoshimura K, Miyamoto F, Kodama E, Harada S, et al. (2011) In vitro and In vivo Resistance to Human Immunodeficiency Virus Type 1 Entry Inhibitors. AIDS Clin Res.
37. Berro R, Klasse PJ, Jakobsen MR, Gorry PR, Moore JP, et al. (2012) V3 determinants of HIV-1 escape from the CCR5 inhibitors Maraviroc and Vicriviroc. Virology 427: 158–165.
38. Yusa K, Maeda Y, Fujioka A, Monde K, Harada S (2005) Isolation of TAK-779-resistant HIV-1 from an R5 HIV-1 GP120 V3 loop library. J Biol Chem 280: 30083–30090.

Journal of General Virology (2013), **94**, 1318–1324 DOI 10.1099/vir.0.050252-0

Short Communication

TRIM5 genotypes in cynomolgus monkeys primarily influence inter-individual diversity in susceptibility to monkey-tropic human immunodeficiency virus type 1

Akatsuki Saito,[1] Masako Nomaguchi,[2] Ken Kono,[3] Yasumasa Iwatani,[4] Masaru Yokoyama,[5] Yasuhiro Yasutomi,[6] Hironori Sato,[5] Tatsuo Shioda,[3] Wataru Sugiura,[4] Tetsuro Matano,[7] Akio Adachi,[2] Emi E. Nakayama[3] and Hirofumi Akari[1]

Correspondence
Hirofumi Akari
akari.hirofumi.5z@kyoto-u.ac.jp
Emi E. Nakayama
emien@biken.osaka-u.ac.jp

[1]Center for Human Evolution Modeling Research, Primate Research Institute, Kyoto University, 41-2 Kanrin, Inuyama, Aichi 484-8506, Japan

[2]Department of Microbiology, Institute of Health Biosciences, University of Tokushima Graduate School, 3-18-15 Kuramoto, Tokushima, Tokushima 770-8503, Japan

[3]Department of Viral Infections, Research Institute for Microbial Diseases, Osaka University, 3-1 Yamadaoka, Suita, Osaka 565-0871, Japan

[4]Clinical Research Center, National Hospital Organization Nagoya Medical Center, 4-1-1 Sannomaru, Naka-ku, Nagoya, Aichi 460-0001, Japan

[5]Laboratory of Viral Genomics, Pathogen Genomics Center, National Institute of Infectious Diseases, 4-7-1 Gakuen, Musashimurayama, Tokyo 208-0011, Japan

[6]Tsukuba Primate Research Center, National Institute of Biomedical Innovation, 1-1 Hachimandai, Tsukuba, Ibaraki 305-0843, Japan

[7]AIDS Research Center, National Institute of Infectious Diseases, 1-23-1 Toyama, Shinjuku-ku, Tokyo 162-8640, Japan

Received 28 November 2012
Accepted 12 March 2013

TRIM5α restricts human immunodeficiency virus type 1 (HIV-1) infection in cynomolgus monkey (CM) cells. We previously reported that a *TRIMCyp* allele expressing TRIM5–cyclophilin A fusion protein was frequently found in CMs. Here, we examined the influence of *TRIM5* gene variation on the susceptibility of CMs to a monkey-tropic HIV-1 derivative (HIV-1mt) and found that TRIMCyp homozygotes were highly susceptible to HIV-1mt not only *in vitro* but also *in vivo*. These results provide important insights into the inter-individual differences in susceptibility of macaques to HIV-1mt.

Considering the global human immunodeficiency virus type 1 (HIV-1) epidemic, development of prophylactic vaccines is strongly desired. In order to evaluate the efficacy of the vaccines, a suitable animal model is also indispensable. However, HIV-1 does not grow in Old World Monkeys (OWMs) such as rhesus monkeys and cynomolgus monkeys (CMs). One of the restriction factors of OWMs is ApoB mRNA editing catalytic subunit 3G (APOBEC3G) (Sheehy *et al.*, 2002). APOBEC3G modifies the minus-strand viral DNA during reverse transcription, resulting in impairment of HIV-1 replication. This activity can be counteracted by the viral protein Vif of simian immunodeficiency virus (SIV) but not by that of HIV-1 (Mariani *et al.*, 2003). Another restriction factor is tripartite motif-containing protein 5α (TRIM5α), which recognizes the viral core and facilitates premature uncoating (Stremlau *et al.*, 2004). To establish a feasible model of HIV-1 infection, monkey-tropic HIV-1 (HIV-1mt) clones were constructed, which were expected to escape from these restriction factors (Hatziioannou *et al.*, 2006; Kamada *et al.*, 2006). In CMs, we reported previously that a modified HIV-1mt, MN4-5S, in which *vif* and the loops of α-helices 4 and 5 (L4/5) and α-helices 6 and 7 of the capsid protein (CA) of HIV-1 were replaced with those of SIVmac239, a pathogenic molecular clone of rhesus macaque SIV, showed enhanced virus replication *in vitro* (Kuroishi *et al.*, 2009) and *in vivo* (Saito *et al.*, 2011).

Accumulating evidence indicates intra-species variations in human and macaque *TRIM5* genes (Johnson & Sawyer, 2009). TRIMCyp is an alternatively spliced isoform of the *TRIM5* gene in which the PRYSPRY domain of TRIM5α is

One supplementary figure is available with the online version of this paper.

replaced with a retrotransposed cyclophilin A (*cypA*) gene (Brennan *et al.*, 2008; Liao *et al.*, 2007; Newman *et al.*, 2008). We recently reported that the frequency of TRIMCyp alleles was >0.8 in Philippine CMs, which is in contrast to the situation in Indochina CMs (Saito *et al.*, 2012a, 2012b). CM TRIMCyp, also known as Mafa TRIMCyp2 (Ylinen *et al.*, 2010), can restrict HIV-1, but fails to do so in SIVmac and HIV-1mt NL-DT5α with L4/5 derived from SIVmac (Saito *et al.*, 2012a), as the CypA domain of CM TRIMCyp binds to L4/5 of HIV-1, but not that of SIVmac (Price *et al.*, 2009; Ylinen *et al.*, 2010).

We recently reported that a new proviral HIV-1mt construct, MN4Rh-3, carrying a glutamine-to-aspartic acid substitution at position 110 (Q110D) of CA in the parental HIV-1mt MN4-8S (Fig. 1), exhibited further enhanced growth properties in a macaque T-cell line (Nomaguchi *et al.*, 2013a, b). In the present study, we investigated whether TRIMCyp alleles in CMs could influence the susceptibility to HIV-1mt infection.

First, we analysed the replication kinetics of HIV-1mt MN4Rh-3 in $CD8^+$ cell-depleted PBMCs from 26 CMs comprising nine TRIM5α homozygotes, eight TRIM5α/TRIMCyp heterozygotes and nine TRIMCyp homozygotes. Prior to this experiment, we confirmed the expression of TRIM5α and/or TRIMCyp in PBMCs from monkeys by reverse transcription-PCR (RT-PCR). We found that the mRNA expression was consistent with the *TRIM5* genotype of each monkey, i.e. the TRIM5α or TRIMCyp homozygotes expressed the respective mRNA, and the heterozygotes expressed both TRIM5α and TRIMCyp mRNAs (Fig. S1, available in JGV Online). Virus stocks for infection experiments were prepared by transfecting HIV-1mt MN4Rh-3 and HIV-1mt MN4-8S clones into HEK293T cells (Saito *et al.*, 2011). Preparation of $CD8^+$ cell-depleted PBMCs and evaluation of viral growth were performed as described previously (Saito *et al.*, 2011). In Fig. 2(a), representative viral kinetics in PBMCs from animals with each *TRIM5* genotype are presented. For comparison, the replication kinetics of HIV-1mt MN4Rh-3 in cells from all 26 animals is shown at the bottom of the figure. Furthermore, the impact of each *TRIM5* genotype on HIV-1mt MN4Rh-3 and MN4-8S replication was evaluated by plotting the peak p24 levels during the observation period (Fig. 2b). HIV-1mt MN4Rh-3 grew significantly better in the PBMCs from TRIMCyp homozygotes or heterozygotes than in those from TRIM5α homozygotes, whilst there was no significant difference between TRIMCyp homozygotes and heterozygotes (Fig. 2a, b). Our results on heterozygotes were consistent with previous findings that co-expression of TRIM5α variants with a distinct antiviral activity interferes with the antiviral activity of the wild-type TRIM5α (Javanbakht *et al.*, 2005; Lim *et al.*, 2010; Nakayama *et al.*, 2006; Perez-Caballero *et al.*, 2005; Stremlau *et al.*, 2004). In addition, HIV-1mt MN4Rh-3 grew better in PBMCs of both TRIMCyp homozygotes and the heterozygotes than HIV-1mt MN4-8S (Fig. 2a, b), which was in agreement with our recent data obtained in a CM-derived T-cell line (Nomaguchi *et al.*, 2013b). Of note, there was no significant difference between each *TRIM5* genotype in the susceptibility to SIVmac239 infection (Fig. 2c), suggesting that the CM *TRIM5* genotypes specifically influence susceptibility to HIV-1mt infection.

We finally investigated whether *TRIM5* genotypes could influence the growth of HIV-1mt MN4Rh-3 *in vivo*. Healthy adult CMs seronegative for B virus and simian retrovirus were housed in individual isolators in a Biosafety Level 3 facility and maintained according to National Institute of Biomedical Innovation guidelines. All experiments were approved by the Animal Welfare and Animal Care Committee of the National Institute of Biomedical Innovation, as well as by Kyoto University. Bleeding and virus inoculation were performed under ketamine hydrochloride anaesthesia. Viral stocks propagated in $CD8^+$ cell-depleted PBMCs were inoculated intravenously into TRIMCyp homozygotes (n=6) or TRIM5α homozygotes (n=3) at a dose of HIV-1mt corresponding to 10 ng CA per head. The profiles of plasma viral loads and anti-HIV-1 antibody responses were evaluated as described previously (Saito *et al.*, 2011). We found that HIV-1mt MN4Rh-3 growth was readily observed in all

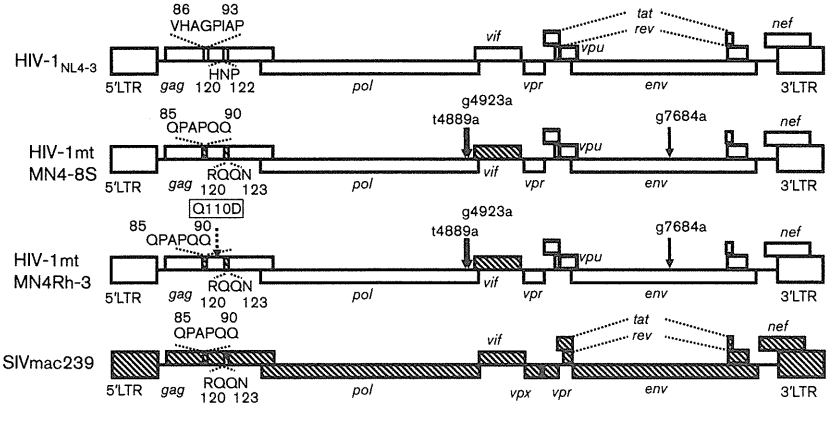

Fig. 1. Structure of the HIV-1mt clones (MN4-8S and MN4Rh-3) used in this study. Open boxes denote HIV-1 (NL4-3) and hatched boxes denote SIVmac239 sequences. Black arrows show adaptive mutations that enhance viral growth potential in CM T-cell lines. Dotted arrows show the CA Q110D mutation.

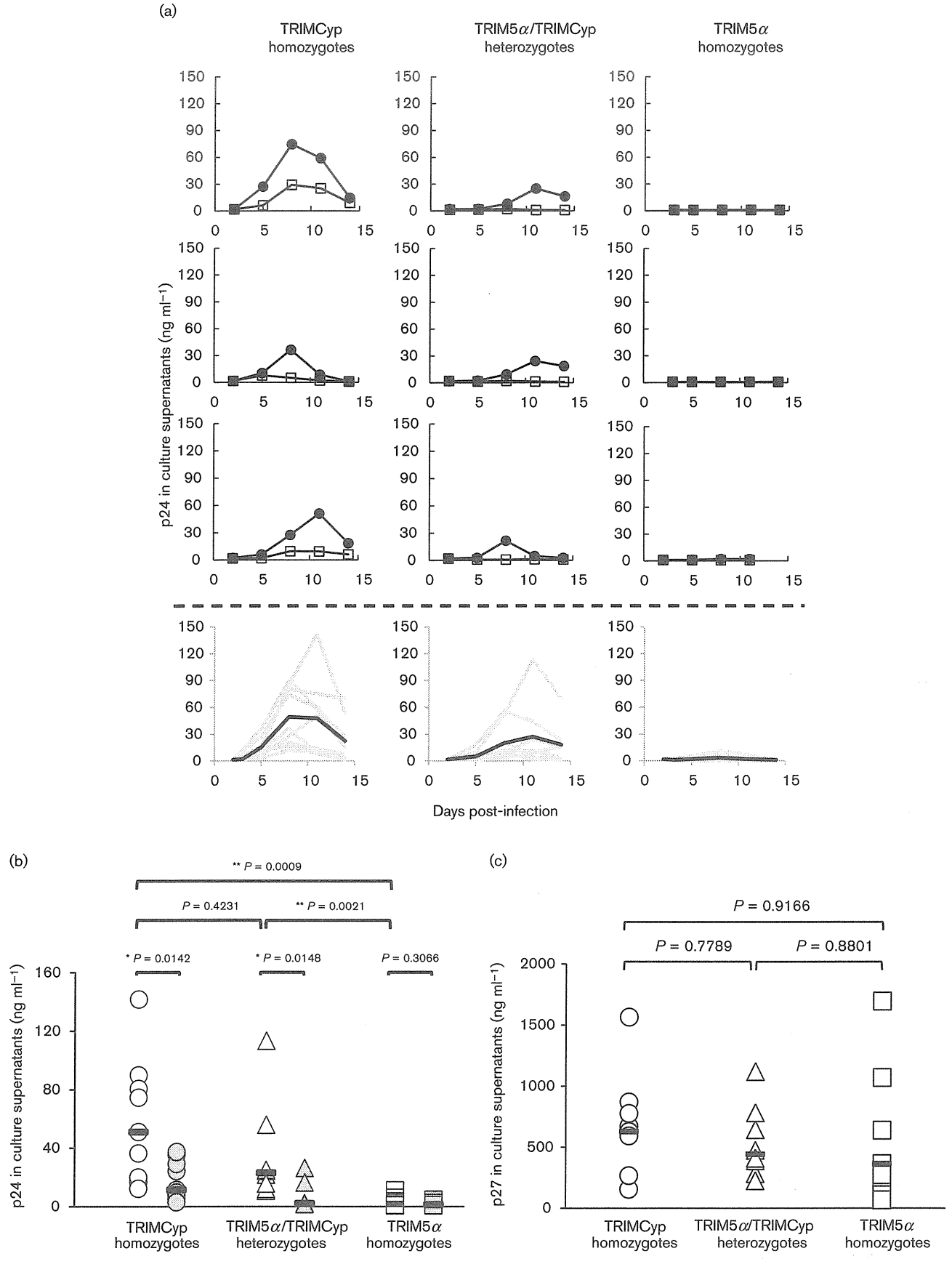
(a)
TRIMCyp homozygotes
TRIM5α/TRIMCyp heterozygotes
TRIM5α homozygotes
p24 in culture supernatants (ng ml−1)
Days post-infection
(b)
** P = 0.0009
P = 0.4231
** P = 0.0021
* P = 0.0142
* P = 0.0148
P = 0.3066
p24 in culture supernatants (ng ml−1)
TRIMCyp homozygotes
TRIM5α/TRIMCyp heterozygotes
TRIM5α homozygotes
(c)
P = 0.9166
P = 0.7789
P = 0.8801
p27 in culture supernatants (ng ml−1)
TRIMCyp homozygotes
TRIM5α/TRIMCyp heterozygotes
TRIM5α homozygotes

Fig. 2. (a) Growth properties of HIV-1mt derivatives in CM PBMCs. $CD8^+$ cell-depleted PBMCs were infected with HIV-1mt MN4Rh-3 (●) or HIV-1mt MN4-8S (□). Culture supernatants were collected periodically and virus replication was assessed using a HIV-1 p24 antigen capture assay kit. These experiments carried out on the PBMCs of each of the 26 macaques were done once. Representative results of virus replication kinetics in the PBMCs prepared from three animals of each *TRIM5* genotype are shown. For comparison, the replication kinetics of HIV-1mt MN4Rh-3 in the PBMCs from the 26 animals are shown at the bottom of the figure (indicated as grey lines). The mean values of the viral growth kinetics in each genotype are indicated in black lines. (b) Influence of *TRIM5* genotypes on the replication of HIV-1mt derivatives in PBMCs. $CD8^+$ cell-depleted PBMCs were infected with HIV-1mt MN4Rh-3 (open symbols) or HIV-1mt MN4-8S (shaded symbols). The cells were derived from TRIMCyp homozygotes ($n=9$), TRIM5α/TRIMCyp heterozygotes ($n=8$) and TRIM5α homozygotes ($n=9$). The peak p24 levels of the virus replication kinetics as shown in Fig. 2(a) were plotted. Thick horizontal bars indicate the median values. Differences in the mean values were assessed using the Wilcoxon rank-sum test (for HIV-1mt MN4Rh-3 and HIV-1mt MN4-8S viruses in each monkey group) and using the Steel–Dwass multiple comparison procedure (for HIV-1mt MN4Rh-3 in the three monkey groups). $^*P<0.05$; $^{**}P<0.01$. (c) Influence of *TRIM5* genotypes on the replication of SIVmac239 in PBMCs. $CD8^+$ cell-depleted PBMCs were infected with SIVmac239. Virus replication was monitored by detecting p27 antigen in the culture supernatants, and the p27 level on the peak day during the observation period (14 days) was plotted. Thick horizontal bars indicate the median values. Differences in the mean values were assessed by the Wilcoxon rank-sum test.

TRIMCyp homozygotes, with plasma viral loads reaching a peak at 2–4 weeks post-inoculation (p.i.) and ranging from 1.1×10^4 to 1.5×10^5 copies ml^{-1} (mean 4.2×10^4 copies ml^{-1}; Fig. 3a). In contrast, HIV-1mt MN4Rh-3 scarcely replicated in TRIM5α homozygotes (mean 1.9×10^3 copies ml^{-1}; Fig. 3a). Accordingly, HIV-1-specific antibodies were also detected in plasma from 3 to 9 weeks p.i. in the TRIMCyp homozygotes but minimally in TRIM5α homozygotes (Fig. 3b), suggesting that the strength of antibody response reflected the level of virus replication. Notably, although TRIMCyp homozygotes had a higher viraemia compared with TRIM5α homozygotes, none developed persistent viraemia (Fig. 3a). As our present HIV-1mts were focused on evasion of TRIM5- and APOBEC3-mediated restrictions, it is reasonable to assume that additional modifications of the viral genome, especially in order to overcome bone marrow stromal antigen 2 (BST-2)-mediated (Jia *et al.*, 2009; Neil *et al.*, 2008; Van Damme *et al.*, 2008) and SAM domain and HD domain-containing protein 1 (SAMHD1)-mediated restriction (Hrecka *et al.*, 2011; Laguette *et al.*, 2011), may be required to establish persistent viraemia *in vivo*. Moreover, Bitzegeio *et al.* (2013) recently suggested the existence of unidentified, type I interferon-inducible antiviral host factors in macaque PBMCs that inhibit HIV-1 replication.

In humans, several genetic factors related to HIV-1 susceptibility have been reported (reviewed by Chatterjee, 2010; Shioda & Nakayama, 2006). A polymorphism in the chemokine (C–C motif) receptor-5 (*CCR5*) gene is an eminent example; thus, individuals carrying a 32 bp deletion in *CCR5* (CCR5-Δ32) are resistant to CCR5-tropic HIV-1 infection and show delayed progression to AIDS (Dean *et al.*, 1996; Samson *et al.*, 1996). In addition to *CCR5*, polymorphisms in the genes encoding IL-4 and IL-10 (Shin *et al.*, 2000) and human leukocyte antigen (Carrington & O'Brien, 2003), as well as *TRIM5* (Sawyer *et al.*, 2006), have also been suggested to affect disease progression in HIV-1-infected individuals. One of the single-nucleotide polymorphisms (SNPs) in human *TRIM5* is a C127T nucleotide substitution, corresponding to an H43Y amino acid substitution in the RING domain. A correlation between this SNP and rapid disease progression has been suggested (van Manen *et al.*, 2008), although this remains controversial (Nakayama *et al.*, 2007; Speelmon *et al.*, 2006). In macaques, an effect of polymorphisms in *TRIM5* on SIV infection has been reported (Kirmaier *et al.*, 2010; Lim *et al.*, 2010); thus, rhesus macaques with TFP residues at positions 339–341 of TRIM5α show greater resistance to SIVsmE041 and SIVsmE543–3 compared with animals with a single glutamine residue at position 339 (Kirmaier *et al.*, 2010). However, it remains elusive as to whether genetic diversity might affect HIV-1mt infection in macaques. In this study, we found for the first time that the *TRIM5* genotypes of CMs primarily influenced inter-individual diversity in terms of susceptibility to HIV-1mt. Our results will provide an important insight into the divergent susceptibility of macaques to HIV-1mt. In particular, the finding that the TRIMCyp homozygotes exhibited a greater susceptibility to HIV-1mt infection will make it possible to identify the susceptibility of each CM by pre-screening for *TRIM5* genotypes, which will be invaluable in establishing a pre-clinical non-human primate model of HIV-1mt infection using CMs. It is noteworthy that our result is consistent with the findings that pig-tailed macaques, a macaque species that is thought to possess TRIMCyp exclusively instead of TRIM5α, shows higher susceptibility to HIV-1 infection (Agy *et al.*, 1992). For this reason, pig-tailed macaques are expected to be a promising model animal for HIV-1mt infection. Indeed, it was reported previously that these macaques developed persistent viraemia following HIV-1mt challenge (Hatziioannou *et al.*, 2009; Igarashi *et al.*, 2007; Thippeshappa *et al.*, 2011).

Moreover, our findings, in which CM *TRIM5* genotype was shown to influence susceptibility to retroviral infection, may imply that the marked geographical variation in the genotypes (Berry *et al.*, 2012; Dietrich *et al.*, 2011; Saito *et al.*, 2012a; Saito *et al.*, 2012b) is a consequence of selective pressures driven by some external factors. As both TRIM5α and TRIMCyp are thought to be associated with retrovirus replication, it is reasonable to speculate that a geographically diverse prevalence of some pathogen(s) such as exogenous or endogenous retroviruses might